Seventh Virial Coefficients for Hard Spheres and Hard Disks*

FRANCIS H. REE AND WILLIAM G. HOOVER
Lawrence Radiation Laboratory, University of California, Livermore, California

(Received 8 September 1966)

The seventh virial coefficient B_7 is expressed as a sum of modified star integrals instead of the usual Mayer star integrals. The new graphs contain both Mayer f functions and $\bar{f}(\equiv 1+f)$ functions. This simplifies the calculation of B_7. That is, instead of the 468 star integrals that appear in Mayer's formulation, only 171 modified star integrals now appear in the evaluation of B_7. Furthermore, for D-dimensional particles with a hard core, these 171 integrals are strongly dependent on the number of dimensions D. For hard rods, hard disks, and hard spheres, respectively, at most one, 78, and 164 of these integrals give a nonvanishing contribution to B_7. When Monte Carlo integration is used to evaluate these integrals using hard-sphere and hard-disk potentials we obtain the following values of B_7: hard spheres, $B_7/(B_2)^6=0.0138\pm0.0004$; hard disks, $B_7/(B_2)^6=0.1141\pm0.0005$. For hard spheres, the truncated seven-term virial series for the pressure agrees within 10% with the results of the molecular dynamics data throughout the fluid phase. The Padé approximants to the pressure obtained from $B_n(n<8)$ data agree even better ($\lesssim 5\%$) with the molecular-dynamics data on the fluid side. Estimated values of $B_8/(B_2)^7$ obtained from the Padé approximants are 0.005 and 0.063 for hard spheres and hard disks, respectively. Furthermore, for hard disks, the Padé approximants obtained from the seven known values of $B_n(n<8)$ indicate that the virial series shows an unstable phase at $\rho=\rho_0$. If this is in fact true, then the low-density study of the equation of state for hard disks would yield some information on the high-density side. We have also calculated the first seven coefficients C_n of the density expansion of the isothermal compressibility for hard spheres, hard disks, hard parallel cubes, and hard parallel squares. We find that these C_n alternate in sign. For two-dimensional continuum particles with a hard core, the corresponding compressibility series appear to converge faster than the usual virial series of the pressure. We also compare the present values of B_7 with the various values of B_7 calculated from approximate theories.

I. INTRODUCTION

THE pressure P for a system of N particles in a volume V at a temperature T can be expanded in the number density $\rho(\equiv N/V)$; i.e.,

$$PV/(NkT)=1+B_2\rho+B_3\rho^2+B_4\rho^3+\cdots, \quad (1)$$

where k is Boltzmann's constant. If the potential energy of the particles is pairwise additive, the nth virial coefficient B_n can be expressed as follows[1]:

$$B_n=[(1-n)/n!](V_n)_n; \quad (2)$$

the notation $(\ )_n$ is used to indicate integration, $(1/V)\int(\ )d\mathbf{r}^n$ over the volume V. The quantity V_n is the sum of all labeled stars[2] with n points. The lines in these stars are Mayer f functions

$$f_{ij}\equiv\exp(-\beta\phi_{ij})-1, \qquad \beta\equiv 1/(kT), \quad (3)$$

where ϕ_{ij} is the pair potential between particles i and j. From experimental values of $PV/(NkT)$, it is possible to obtain experimental values of the virial coefficients by fitting the data with a truncated density series (1). If these experimental virial coefficients are next used to fit theoretical virial coefficients calculated from (2) by using a given pair potential with several adjustable parameters, some useful knowledge on the possible shape of the potential can be deduced. However, the above approach has had only limited success. Even for inert gases,[3] the experimental data have not been accurately determined over the wide ranges of temperatures and densities necessary to estimate coefficients beyond B_3. Theoretical calculations of the virial coefficients are limited by our lack of knowledge of an accurate pair potential. Although the pairwise additivity assumption is no doubt sufficient to describe the equilibrium behavior of an inert gas liquid state,[4,5] even in the absence of many-body forces, the third and higher virial coefficients depend sensitively on the shape of the potential. There is little doubt, however, that a pair potential *could* be found to fit B_2 and B_3 simultaneously.

One reason for calculating virial coefficients beyond B_3 for an *idealized* pair potential is to check the accuracy of approximate theories of fluids by using an *idealized* pair potential. An improved version[6] of an approximate theory often is accompanied by improved values of the first few B_n's so that the calculation of the higher B_n becomes useful to check the accuracy of the improved theory. Another reason for evaluating higher B_n is to determine the density region in which the virial ex-

* This work was performed under the auspices of the U.S. Atomic Energy Commission.

[1] J. E. Mayer and M. G. Mayer, *Statistical Mechanics* (John Wiley & Sons, Inc., New York, 1940).

[2] We follow the graph theoretical terminologies used by G. E. Uhlenbeck and G. W. Ford, in *Studies in Statistical Mechanics*, J. de Boer and G. E. Uhlenbeck, Eds. (North-Holland Publ. Co., Amsterdam, 1962), Vol. 1, Pt. B.

[3] J. O. Hirschfelder, C. F. Curtiss, and R. B. Bird, *Molecular Theory of Gases and Liquids* (John Wiley & Sons, Inc., New York, 1954), Chap. 3.

[4] E. A. Guggenheim, J. Chem. Phys. **13**, 253 (1945).

[5] R. N. Keeler, M. Van Thiel, and B. J. Alder, Physica **31**, 1437 (1965).

[6] For example, see L. Verlet, Physica **30**, 95 (1964).

pansion converges. A rigorous lower bound on the virial series radius of convergence has been recently established.[7] For hard spheres, this lower bound corresponds to about 0.026 of the close-packed density. This value however, appears to lie far below the actual radius of convergence, since a truncated virial series[8] for hard spheres agrees within several percent with the data obtained from the molecular dynamics[9] or Monte Carlo calculations[10] over the entire fluid range. Padé approximants[8] to the pressure for hard spheres and hard disks constructed from the first few known virial coefficients are known to agree also within experimental accuracy of the data obtained by molecular dynamic calculations on the fluid phase. Therefore, they might also provide useful information on the true radius of convergence.

The hard-sphere potential is a suitable choice for evaluating higher virial coefficients for two reasons. First, the various integrals occurring in the expression of B_n are easily evaluated for hard spheres. Second, any physical phenomenon occurring at high densities or high temperatures for a system of particles such as argon atoms can be described fairly adequately with only the repulsive part of the pair potential used.

The following values of B_n's ($n<7$) for hard spheres and hard disks have been evaluated[8,11]:

Hard spheres:

$$B_2\equiv b=\tfrac{2}{3}\pi\sigma^3,$$

$$B_3/b^2=\tfrac{5}{8},$$

$$\frac{B_4}{b^3}=-\frac{89}{280}+\frac{219\sqrt{2}}{2240\pi}+\frac{4131}{2240\pi}\cos^{-1}\left(\frac{1}{\sqrt{3}}\right)=0.28695,$$

$$B_5/b^4=0.1103\pm0.0003,\text{ and }B_6/b^5=0.0386\pm0.0004; \tag{4}$$

Hard disks:

$$B_2\equiv b=\tfrac{1}{2}\pi\sigma^3,$$

$$B_3/b^2=\tfrac{4}{3}-(\sqrt{3}/\pi)=0.78200,$$

$$B_4/b^3=2-\tfrac{9}{2}(\sqrt{3}/\pi)+(10/\pi^2)=0.53223,$$

$$B_5/b^4=0.3338\pm0.0005,\text{ and }B_6/b^5=0.1992\pm0.0008, \tag{5}$$

where σ is sphere or disk diameter. The values of B_5 and B_6 in (4) and (5) were obtained by using Monte Carlo integration of the various integrals appearing in (2).

Calculating higher B_n becomes increasingly difficult, since we must consider a larger number of star integrals, each of which becomes harder to evaluate as n becomes large. Moreover, approximately half the star integrals are positive, and the remaining half are negative. B_n is the small residue remaining after extensive cancellation in adding up the positive and negative star integrals. In order partially to avoid these difficulties, we have previously[12] reformulated the usual graphical representation of the virial series in terms of graphs containing not only Mayer f functions, but also $\bar{f}$ functions defined by

$$\bar{f}\equiv 1+f=\exp(-\beta\phi). \tag{6}$$

The reformulation has two advantages over the usual Mayer formulation: The number of topologically different graphs contributing to B_n is reduced and, for hard potentials, these modified star integrals depend strongly on the dimensionality of the system. If B_7 is expressed in terms of the modified stars occurring in the reformulated expression of B_7, only 171 modified star integrals contribute to B_7; in contrast there are 468 star integrals occurring in the Mayer formulation of B_7. For one-dimensional hard rods, only one (complete star integral) out of the 171 modified star integrals makes a nonvanishing contribution to B_7. In the following section, we briefly sketch the reformulation of the virial series and describe the method used to obtain the 171 modified star integrals. In Sec. III, we show how these integrals depend on dimensionality if a hard-core potential is used. In Sec. IV, a Monte Carlo method is used to evaluate all modified star integrals occurring in the expression of B_7 for hard spheres and hard disks. The radius of convergence of the virial series is reserved for discussion in Sec. V.

II. REFORMULATED EXPRESSION FOR B_7

The Mayer expression for $(V_n)_n$ in (2) can be expressed as

$$(V_n)_n=\sum_{i=1}^{S^{n\ddagger}}\mathfrak{s}_i[n](S_i[n])_n, \tag{7}$$

where $\mathfrak{s}_i[n]$ is the number of ways an n-point star of the ith-type $S_i[n]$ can be labeled, and $S^{n\ddagger}$ denotes the total number of different types of n-point stars.[13] In a previous publication,[12] an alternate expression for $(V_n)_n$ was obtained; i.e.,

$$(V_n)_n=\sum_{i=1}^{S^{n\ddagger}}\mathfrak{s}_i[n]\tilde{a}_i[n](\tilde{S}_i[n])_n, \tag{8}$$

[7] J. L. Lebowitz and O. Penrose, J. Math. Phys. **5**, 841 (1964). The bound given in this paper can be slightly improved for repulsive potentials [see F. H. Ree, Phys. Rev. **155**, 84 (1967)].

[8] F. H. Ree and W. G. Hoover, J. Chem. Phys. **40**, 939 (1964).

[9] B. J. Alder and T. E. Wainwright, J. Chem. Phys. **33**, 1439 (1960).

[10] W. W. Wood and J. D. Jacobson, J. Chem. Phys. **27**, 1207 (1957).

[11] See the references quoted in Ref. 8. The exact value of the hard-disk B_4 is obtained recently by J. S. Rowlinson, Mol. Phys. **7**, 593 (1963–1964); and P. C. Hemmer, J. Chem. Phys. **42**, 1116 (1965). The hard-sphere B_5 quoted in Eq. (4) agrees with the calculations of S. Katsura and Y. Abe, J. Chem. Phys. **39**, 2068 (1963); J. S. Rowlinson, Proc. Roy. Soc. (London) **A279**, 147 (1964); and those of F. H. Ree, R. N. Keeler, and S. L. McCarthy, J. Chem. Phys. **44**, 3407 (1966) within each other's error bounds.

[12] F. H. Ree and W. G. Hoover, J. Chem. Phys. **41**, 1635 (1964).

[13] For graphical notations used in this section, we refer to Ref. 12.

where $\tilde{S}_i[n]$ is the ith type of n-point modified star, obtained from $S_i[n]$ by connecting with $\tilde{f}$ functions all pairs of points which are not connected by f functions. The quantity $\tilde{a}_i[n]$ was defined as the *star content* of an n-point modified star of the ith type. It can be obtained by using the following recipe: *Count the number of labeled Mayer stars which can be formed by successively removing* 0, 2, 4$\cdots$*f functions from the f functions of any star* $S_i[\mathbf{r}^n]$ *of type* $S_i[n]$*; then subtract the number of labeled Mayer stars which can be formed by removing* 1, 3, 5, $\cdots$*f functions from the f functions of the same star. The resulting number is* $\tilde{a}_i[n]$. The star content can be positive, negative, or zero. An alternate procedure for establishing the relationship (8) is to introduce the factor $\tilde{f}-f(\equiv 1)$ between every pair of points in $S_i[\mathbf{r}^n]$ which are not connected by a Mayer f function. When these factors are expanded, the Mayer star $S_i[\mathbf{r}^n]$ can be expressed as a sum of modified stars of $\tilde{S}_j[\mathbf{r}^n]$. When this process is applied to all Mayer stars occurring in (7), and the resulting expression (7) is written as a sum over modified stars, (8) is obtained. For the four-, five-, and six-point stars, the transformation to the modified stars by the latter method can be accomplished in a simple manner, and these are given in Ref. 8. From the transformation tables of Ref. 8, we then find that there are 5 five-point and 33 six-point modified stars with zero star content. Therefore, we need not evaluate the corresponding modified star integrals in calculating B_5 and B_6. To construct an analogous transformation table for the 468 topologically different seven-point Mayer stars, and also to evaluate the star content for all seven-point modified stars, we adopt the following systematic method: First, 21 binary bits (1 or 0) are used to specify

TABLE I. Values of B_7 and the seven-point modified star integrals with nonzero star contents for hard spheres and hard disks.

i^a	Star	Coefficient in B_7/b^6	Unlabeling factor[b]	Values[c] of the integrals f/b^6 Spheres	Disks	Contribution to B_7/b^6 Spheres	Disks
1 (1)		-360	1	$-(1.95\pm0.04)\times10^{-2}$	$-(7.3\pm0.2)\times10^{-3}$	+0.0084	+0.0031
2 (4)		-1260	3	$+(2.2\pm0.2)\times10^{-4}$	negligible	-0.0003	-0.0000
3 (5)		-1260	3	$+(1.3\pm0.1)\times10^{-4}$	negligible	-0.0002	-0.0000
4 (14)		-420	0	negligible	0	+0.0000	+0.0000
5 (15)		2520	9	$-(3.17\pm0.05)\times10^{-3}$	$-(1.98\pm0.03)\times10^{-3}$	-0.0095	-0.0059
6 (20)		-630	1	negligible	0	+0.0000	+0.0000
7 (21)		10080	30	$-(1.38\pm0.06)\times10^{-4}$	$-(1.4\pm0.2)\times10^{-5}$	-0.0017	-0.0002
8 (22)		1260	0	$-(8\pm3)\times10^{-6}$	0	-0.0000	-0.0000
9 (23)		1680	4	$-(1.8\pm0.5)\times10^{-5}$	negligible	-0.0000	-0.0000
10 (24)		1680	4	$-(6\pm1)\times10^{-5}$	negligible	-0.0001	-0.0000
11 (25)		2520	14	$-(1.3\pm0.2)\times10^{-5}$	0	-0.0000	-0.0000
12 (26)		-21	0	negligible	0	-0.0000	-0.0000
13 (52)		2520	6	$+(2.2\pm0.4)\times10^{-5}$	0	+0.0001	+0.0000
14 (53)		630	3	negligible	0	+0.0000	+0.0000
15 (58)		-7560	29	$+(1.05\pm0.01)\times10^{-3}$	$+(6.9\pm0.1)\times10^{-4}$	-0.0095	-0.0062
16 (61)		5040	8	$\sim+10^{-6}$	0	+0.0000	+0.0000
17 (65)		2520	8	$+(2.0\pm0.4)\times10^{-5}$	0	+0.0001	+0.0000
18 (66)		-2520	28	$+(3.4\pm0.3)\times10^{-5}$	0	-0.0001	-0.0000
19 (67)		-7560	26	$+(1.34\pm0.06)\times10^{-4}$	$+(8.0\pm0.3)\times10^{-5}$	-0.0012	-0.0005
20 (68)		-3780	13	$+(6.5\pm0.6)\times10^{-5}$	$+(1.7\pm0.2)\times10^{-5}$	-0.0003	-0.0001
21 (69)		-5040	44	$+(2.3\pm0.2)\times10^{-5}$	0	-0.0001	-0.0000
22 (70)		-5040	50	$+(4.5\pm0.8)\times10^{-6}$	0	-0.0000	-0.0000
23 (72)		2520	20	$+(2.4\pm0.6)\times10^{-5}$	0	+0.0000	-0.0000
24 (73)		-5040	15	$+(5.1\pm0.4)\times10^{-5}$	$+(1.3\pm0.6)\times10^{-6}$	-0.0003	-0.0000
25 (74)		-5040	30	$+(7\pm1)\times10^{-6}$	0	-0.0000	-0.0000
26 (75)		-1890	9	negligible	0	-0.0000	-0.0000
27 (76)		420	0	negligible	0	-0.0000	-0.0000
28 (121)		-1260	6	negligible	0	+0.0000	+0.0000
29 (125)		-3780	17	$-(4.3\pm0.4)\times10^{-5}$	0	+0.0002	+0.0000
30 (126)		-3780	11	$-(8\pm1)\times10^{-6}$	0	+0.0000	+0.0000
31 (132)		10080	42	$-(4.32\pm0.08)\times10^{-4}$	$-(3.191\pm0.06)\times10^{-4}$	+0.0052	+0.0038
32 (134)		-2520	32	$\sim-10^{-7}$	0	+0.0000	+0.0000
33 (135)		-15120	56	$-(4.8\pm0.7)\times10^{-6}$	0	+0.0001	+0.0000
34 (136)		-5040	10	negligible	0	+0.0000	+0.0000
35 (139)		-1260	11	$\sim-10^{-6}$	0	+0.0000	+0.0000
36 (140)		2520	34	$-(6\pm1)\times10^{-6}$	0	-0.0000	-0.0000
37 (142)		-10080	36	$-(1.9\pm0.2)\times10^{-5}$	$-(8\pm3)\times10^{-7}$	+0.0002	+0.0000
38 (143)		2520	46	$-(2.05\pm0.05)\times10^{-4}$	$-(1.05\pm0.03)\times10^{-4}$	-0.0006	-0.0003
39 (144)		-2520	12	$-(4.6\pm0.1)\times10^{-4}$	$+(3.4\pm0.1)\times10^{-4}$	+0.0016	+0.0010
40 (145)		5040	94	$-(1.7\pm0.1)\times10^{-5}$	$-(1.9\pm0.9)\times10^{-6}$	-0.0001	-0.0000
41 (147)		5040	86	$-(1.3\pm0.1)\times10^{-5}$	$-(2\pm1)\times10^{-7}$	-0.0001	-0.0000
42 (149)		-10080	80	$-(1.1\pm0.1)\times10^{-5}$	0	+0.0001	+0.0000
43 (151)		-7560	35	negligible	0	+0.0000	+0.0000
44 (153)		-1680	6	0	0	+0.0000	+0.0000
45 (154)		-2520	46	$\sim-10^{-6}$	0	+0.0000	+0.0000
46 (155)		5040	52	$-(2.7\pm0.2)\times10^{-5}$	$-(1.3\pm0.3)\times10^{-6}$	-0.0002	-0.0000
47 (156)		-1260	27	$-(1.1\pm0.5)\times10^{-6}$	negligible	+0.0000	+0.0000
48 (157)		1260	30	negligible	0	-0.0000	-0.0000
49 (179)		-1890	3	negligible	0	-0.0000	-0.0000
50 (184)		-1260	3	negligible	0	-0.0000	-0.0000
51 (186)		2520	11	$+(6.9\pm0.2)\times10^{-4}$	$+(5.6\pm0.2)\times10^{-4}$	+0.0021	+0.0017
52 (211)		1890	14	$+(1.7\pm0.9)\times10^{-6}$	0	+0.0000	+0.0000
53 (212)		-2100	10	$+(9.0\pm0.3)\times10^{-4}$	$+(8.1\pm0.2)\times10^{-4}$	-0.0023	-0.0020
54 (213)		7560	24	$+(7\pm1)\times10^{-6}$	$+(1.2\pm0.5)\times10^{-6}$	+0.0001	+0.0000
55 (221)		5040	88	$+(6\pm2)\times10^{-7}$	0	+0.0000	+0.0000
56 (222)		10080	50	$+(1.6\pm0.1)\times10^{-5}$	0	+0.0002	+0.0000
57 (223)		10080	58	$+(1.2\pm0.1)\times10^{-5}$	0	+0.0001	+0.0000
58 (225)		3360	12	negligible	0	+0.0000	+0.0000
59 (227)		1260	28	negligible	0	+0.0000	+0.0000
60 (228)		2520	20	$+(3.3\pm0.1)\times10^{-4}$	$+(2.53\pm0.06)\times10^{-4}$	+0.0010	+0.0008
61 (230)		5040	72	$+(2.0\pm0.4)\times10^{-5}$	0	+0.0000	+0.0000
62 (231)		25200	136	$+(2.23\pm0.09)\times10^{-5}$	$+(2.9\pm0.3)\times10^{-6}$	+0.0007	+0.0001
63 (232)		2520	30	$+(7\pm1)\times10^{-6}$	0	+0.0000	+0.0000
64 (233)		10080	74	$+(8.5\pm0.8)\times10^{-6}$	$+(5\pm2)\times10^{-7}$	+0.0001	+0.0000
65 (234)		1260	31	$+(2.9\pm0.6)\times10^{-6}$	0	+0.0000	+0.0000
66 (235)		30240	116	$+(1.4\pm0.3)\times10^{-6}$	0	+0.0001	+0.0000
67 (236)		5040	34	negligible	0	+0.0000	+0.0000
68 (237)		-5040	142	$+(6.2\pm0.1)\times10^{-5}$	$+(3.0\pm0.1)\times10^{-5}$	-0.0004	-0.0002
69 (238)		7560	37	$+(1.36\pm0.05)\times10^{-4}$	$+(1.12\pm0.04)\times10^{-4}$	+0.0012	+0.0010
70 (239)		12600	67	$\sim+10^{-7}$	negligible	+0.0000	+0.0000
71 (242)		5040	74	$+(8\pm2)\times10^{-7}$	0	+0.0000	+0.0000
72 (243)		10080	82	$+(8.5\pm0.3)\times10^{-5}$	$+(4.0\pm0.2)\times10^{-5}$	+0.0010	+0.0008
73 (246)		25200	156	$+(4.0\pm0.4)\times10^{-6}$	negligible	+0.0001	+0.0000
74 (246)		2520	44	$+(3.7\pm0.8)\times10^{-6}$	$+(4\pm2)\times10^{-7}$	+0.0000	+0.0000
75 (247)		7560	38	negligible	0	+0.0000	+0.0000
76 (248)		5720	28	$+(5.2\pm0.9)\times10^{-6}$	negligible	+0.0000	+0.0000
77 (249)		6300	44	0	0	+0.0000	+0.0000
78 (250)		10080	92	negligible	0	-0.0000	+0.0000
79 (251)		595	7	0	0	+0.0000	+0.0000
80 (267)		1260	3	negligible	0	-0.0000	-0.0000
81 (277)		1680	6	negligible	0	-0.0000	-0.0000
82 (290)		6300	28	$\sim-10^{-6}$	0	-0.0000	-0.0000
83 (299)		-20160	110	$-(2.04\pm0.03)\times10^{-4}$	$-(1.85\pm0.03)\times10^{-4}$	+0.0049	+0.0044
84 (300)		3780	19	$-(1.0\pm0.6)\times10^{-7}$	0	-0.0000	-0.0000
85 (301)		-2520	52	$-(5\pm1)\times10^{-6}$	0	+0.0000	+0.0000
86 (303)		-5040	52	$-(1.9\pm0.4)\times10^{-6}$	0	+0.0000	+0.0000
87 (305)		-40320	196	$-(1.60\pm0.07)\times10^{-5}$	$-(2.5\pm0.03)\times10^{-6}$	+0.0006	+0.0001
88 (306)		-10080	84	$-(1.1\pm0.1)\times10^{-6}$	0	+0.0000	+0.0000
89 (307)		-8300	44	$-(2.9\pm0.2)\times10^{-5}$	0	+0.0002	+0.0000
90 (309)		-7560	90	$-(3\pm2)\times10^{-7}$	0	+0.0000	+0.0000

TABLE I (*Continued*)

I[a]	Star	Coefficient in B_7X 840	Unlabeling factor[b]	Values of the integrals f_7[c] Spheres	Disks	Contribution to B_7/b^6 Spheres	Disks
91 (312)		-2520	90	$-(7 \pm 2) \times 10^{-7}$	0	+0.0000	+0.0000
92 (315)		-630	3	negligible	0	+0.0000	+0.0000
93 (316)		-13860	55	$-(1.8 \pm 0.4) \times 10^{-5}$	0	+0.0000	+0.0000
94 (317)		-17640	118	$-(1.07 \pm 0.02) \times 10^{-4}$	$-(8.4 \pm 0.2) \times 10^{-5}$	+0.0022	+0.0018
95 (318)		-15120	126	$-(8.4 \pm 0.2) \times 10^{-5}$	$-(7.5 \pm 0.2) \times 10^{-5}$	+0.0015	+0.0014
96 (319)		-10080	220	$-(3.6 \pm 0.3) \times 10^{-6}$	0	+0.0000	+0.0000
97 (320)		-2520	106	$-(6.3 \pm 0.8) \times 10^{-6}$	$-(1.4 \pm 0.3) \times 10^{-6}$	+0.0000	+0.0000
98 (321)		-12600	108	$-(5 \pm 2) \times 10^{-7}$	0	+0.0000	+0.0000
99 (322)		-20160	112	$-(5.1 \pm 0.6) \times 10^{-6}$	negligible	+0.0001	+0.0000
100 (323)		-35280	245	$-(4.2 \pm 0.3) \times 10^{-6}$	$-(3.2 \pm 0.5) \times 10^{-7}$	+0.0002	+0.0000
101 (324)		-17640	120	$-(2.4 \pm 0.3) \times 10^{-6}$	0	+0.0001	+0.0000
102 (325)		-12600	128	$\sim -10^{-7}$	0	+0.0000	+0.0000
103 (326)		-22680	129	$-(1.31 \pm 0.07) \times 10^{-5}$	$-(6.9 \pm 0.4) \times 10^{-6}$	+0.0004	+0.0002
104 (327)		-12600	68	$-(2.9 \pm 0.5) \times 10^{-6}$	negligible	+0.0000	+0.0000
105 (328)		-5040	68	$-(1.2 \pm 0.4) \times 10^{-6}$	0	+0.0000	+0.0000
106 (329)		-20160	69	$-(6.0 \pm 0.7) \times 10^{-6}$	negligible	+0.0001	+0.0000
107 (330)		-30240	135	$-(6 \pm 2) \times 10^{-7}$	0	+0.0000	+0.0000
108 (331)		-3780	12	0	0	+0.0000	+0.0000
109 (332)		-8190	38	0	0	+0.0000	+0.0000
110 (354)		-10080	50	$+(1.8 \pm 0.4) \times 10^{-6}$	0	-0.0000	-0.0000
111 (355)		-525	3	negligible	0	+0.0000	+0.0000
112 (361)		15120	81	$+(1.33 \pm 0.03) \times 10^{-4}$	$+(1.30 \pm 0.03) \times 10^{-4}$	+0.0024	+0.0023
113 (364)		10080	146	$+(6.4 \pm 0.5) \times 10^{-6}$	0	+0.0001	+0.0000
114 (366)		-1260	16	negligible	0	-0.0000	-0.0000
115 (367)		-2520	13	$+(3.8 \pm 0.5) \times 10^{-5}$	$+(4.7 \pm 0.4) \times 10^{-5}$	-0.0001	-0.0001
116 (368)		-8820	64	$\sim +10^{-7}$	0	-0.0000	-0.0000
117 (369)		12600	84	$+(4.75 \pm 0.06) \times 10^{-4}$	$+(5.65 \pm 0.06) \times 10^{-4}$	+0.0071	+0.0085
118 (373)		25200	164	$+(1.97 \pm 0.09) \times 10^{-5}$	$+(1.8 \pm 0.2) \times 10^{-6}$	+0.0006	+0.0000
119 (375)		3150	43	$+(7 \pm 3) \times 10^{-7}$	0	+0.0000	+0.0000
120 (376)		5040	180	$+(2.8 \pm 0.1) \times 10^{-5}$	$+(1.62 \pm 0.06) \times 10^{-5}$	+0.0002	+0.0001
121 (377)		-10060	79	$+(1.5 \pm 0.3) \times 10^{-6}$	0	-0.0000	-0.0000
122 (378)		27720	183	$+(7.5 \pm 0.2) \times 10^{-5}$	$+(6.4 \pm 0.1) \times 10^{-5}$	+0.0025	+0.0021
123 (379)		10080	180	$+(2.2 \pm 0.2) \times 10^{-6}$	0	+0.0000	+0.0000
124 (380)		7560	169	$+(1.7 \pm 0.3) \times 10^{-6}$	$+(8 \pm 2) \times 10^{-7}$	+0.0000	+0.0000
125 (381)		27720	194	$+(3.74 \pm 0.09) \times 10^{-5}$	$+(2.75 \pm 0.08) \times 10^{-5}$	+0.0012	+0.0009
126 (382)		25200	354	$+(1.9 \pm 0.2) \times 10^{-6}$	0	+0.0001	+0.0000
127 (383)		2520	42	$\sim +10^{-6}$	0	+0.0000	+0.0000
128 (384)		7560	100	$+(9 \pm 2) \times 10^{-7}$	0	+0.0000	+0.0000
129 (385)		10080	196	$+(9.7 \pm 0.5) \times 10^{-6}$	$+(7.6 \pm 0.4) \times 10^{-6}$	+0.0001	+0.0001
130 (386)		35280	200	$+(7.3 \pm 0.5) \times 10^{-6}$	$+(8 \pm 2) \times 10^{-7}$	+0.0003	+0.0000
131 (387)		40320	210	$+(4.6 \pm 0.4) \times 10^{-6}$	$+(1.4 \pm 0.6) \times 10^{-7}$	+0.0002	+0.0000
132 (388)		30240	208	$+(4 \pm 1) \times 10^{-7}$	0	+0.0000	+0.0000
133 (389)		7980	38	0	0	+0.0000	+0.0000
134 (390)		1260	10	negligible	0	+0.0000	+0.0000
135 (391)		7920	33	$\sim +10^{-6}$	$+(3 \pm 2) \times 10^{-7}$	+0.0000	+0.0000
136 (405)		7560	48	$+(9.4 \pm 0.9) \times 10^{-6}$	0	-0.0001	+0.0000
137 (408)		6300	48	$+(3.4 \pm 0.5) \times 10^{-6}$	0	-0.0000	+0.0000
138 (413)		13860	115	$+(3.9 \pm 0.5) \times 10^{-6}$	0	-0.0001	+0.0000
139 (415)		-37800	266	$-(2.10 \pm 0.02) \times 10^{-4}$	$-(2.09 \pm 0.02) \times 10^{-4}$	+0.0004	+0.0004
140 (416)		-12600	250	$-(7.1 \pm 0.4) \times 10^{-6}$	0	+0.0001	+0.0000
141 (417)		17640	134	$-(1.77 \pm 0.09) \times 10^{-5}$	$-(1.21 \pm 0.06) \times 10^{-5}$	-0.0004	-0.0003
142 (419)		-20160	568	$-(1.74 \pm 0.04) \times 10^{-5}$	$-(9.3 \pm 0.3) \times 10^{-6}$	+0.0004	+0.0002
143 (420)		-15120	288	$-(1.50 \pm 0.06) \times 10^{-5}$	$-(9.6 \pm 0.4) \times 10^{-6}$	+0.0003	+0.0002
144 (421)		8820	134	$+(1.4 \pm 0.8) \times 10^{-7}$	0	-0.0000	-0.0000
145 (422)		-2520	146	$-(9 \pm 2) \times 10^{-7}$	0	+0.0000	+0.0000
146 (423)		-8400	50	$-(1.5 \pm 0.1) \times 10^{-5}$	$-(6 \pm 2) \times 10^{-7}$	+0.0001	+0.0000
147 (424)		-840	18	negligible	0	+0.0000	+0.0000
148 (425)		1260	40	$-(1.5 \pm 0.2) \times 10^{-5}$	$-(1.7 \pm 0.1) \times 10^{-5}$	-0.0000	-0.0000
149 (426)		-1400	0	0	0	+0.0000	+0.0000
150 (427)		-1260	31	$-(3.7 \pm 0.8) \times 10^{-6}$	negligible	+0.0000	+0.0000
151 (428)		-27720	323	$-(3.0 \pm 0.3) \times 10^{-6}$	$-(1.0 \pm 0.1) \times 10^{-6}$	+0.0001	+0.0000
152 (429)		-5460	56	negligible	0	+0.0000	+0.0000
153 (433)		-2520	13	$+(1.62 \pm 0.08) \times 10^{-4}$	$+(1.45 \pm 0.08) \times 10^{-4}$	-0.0005	-0.0004
154 (440)		-18900	180	$+(1.23 \pm 0.05) \times 10^{-5}$	0	-0.0003	-0.0000
155 (441)		5040	39	$+(6.9 \pm 0.1) \times 10^{-6}$	$+(1.05 \pm 0.01) \times 10^{-3}$	+0.0042	+0.0063
156 (442)		-22680	204	$+(2.45 \pm 0.09) \times 10^{-5}$	$+(1.59 \pm 0.06) \times 10^{-5}$	-0.0007	-0.0004
157 (443)		-6300	51	$+(1.05 \pm 0.03) \times 10^{-4}$	$+(1.24 \pm 0.04) \times 10^{-4}$	-0.0008	-0.0010
158 (444)		-5040	74	$+(3.0 \pm 0.1) \times 10^{-5}$	$+(3.6 \pm 0.2) \times 10^{-5}$	-0.0002	-0.0002
159 (445)		12600	430	$+(5.58 \pm 0.08) \times 10^{-5}$	$+(4.77 \pm 0.07) \times 10^{-5}$	+0.0008	+0.0007
160 (447)		-17640	229	$+(6.2 \pm 0.4) \times 10^{-6}$	$+(8 \pm 4) \times 10^{-6}$	-0.0001	-0.0000
161 (448)		-7560	238	$+(8.3 \pm 0.5) \times 10^{-6}$	$+(7.5 \pm 0.4) \times 10^{-6}$	-0.0001	-0.0001
162 (449)		-2100	19	negligible	0	+0.0000	+0.0000
163 (454)		12600	95	$-(2.1 \pm 0.04) \times 10^{-4}$	$-(2.73 \pm 0.04) \times 10^{-4}$	-0.0032	+0.0041
164 (456)		4200	48	$-(1.5 \pm 0.1) \times 10^{-5}$	0	-0.0001	+0.0000
165 (457)		31500	318	$-(6.9 \pm 0.1) \times 10^{-5}$	$-(5.8 \pm 0.1) \times 10^{-5}$	-0.0026	-0.0021
166 (458)		12600	165	$-(9.7 \pm 0.2) \times 10^{-5}$	$-(1.26 \pm 0.02) \times 10^{-4}$	-0.0015	+0.0019
167 (459)		15750	87	$-(9.3 \pm 0.8) \times 10^{-6}$	$\sim -10^{-7}$	-0.0002	+0.0000
168 (463)		25200	228	$+(4.24 \pm 0.03) \times 10^{-4}$	$+(7.21 \pm 0.04) \times 10^{-4}$	-0.0127	+0.0216
169 (464)		-8400	41	$+(4.0 \pm 0.3) \times 10^{-5}$	$+(4.8 \pm 0.8) \times 10^{-6}$	-0.0006	+0.0006
170 (460)		6300	58	$-(1.53 \pm 0.01) \times 10^{-3}$	$-(3.06 \pm 0.01) \times 10^{-3}$	-0.0115	+0.0230
171 (468)		-420	1	$-(1.53 \pm 0.01) \times 10^{-1}$	$-(9.82 \pm 0.02) \times 10^{-1}$	+0.0223	+0.1430
Values for B_7/b^6:				+0.0138±0.0004	+0.1141±0.0005	+0.0135	+0.1141

[a] The number inside of parentheses represents the ordering of stars given in the Appendix.

[b] The unlabeling factor is the number of ways a modified star graph can be labeled and still satisfy the Monte Carlo trial configurations, $f_{12}=f_{23}=f_{34}=f_{45}=f_{56}=f_{61}=-1$.

[c] B_7 and the modified star integrals for spheres (disks) are calculated from 105 (130) independent batches, each of which contains 50 000 Monte Carlo trial configurations. Each modified star integral is the average of a number (unlabeling factor) of topologically identical but differently labeled star integrals. This is equivalent to evaluating a particular labeled star integral using a number of trial configurations equal to (50 000×unlabeling factor) for each batch. When no configuration corresponding to a particular modified star occurs during the total Monte Carlo trials, the integral B_7 is "negligible." When only one such configuration occurs, the value of the integral is preceded by $\sim$. This is indicated in the columns 5 and 6.

either the presence (1) or the absence (0) of each Mayer f function occurring in the configuration specified by each of the 468 stars. The binary digits are ordered as follows:

$$f_{12}f_{13}f_{14}f_{15}f_{16}f_{17}f_{23}f_{24}f_{25}f_{26}f_{27}f_{34}f_{35}f_{36}f_{37}f_{45}f_{46}f_{47}f_{56}f_{57}f_{67}. \tag{9}$$

Second, each of these 468 stars is uniquely characterized (independent of labeling it) by the following set of numbers: (1) number of f functions, (2) degrees (number of f functions) of each of the seven points, (3) five graph determinants describing complexity of the stars (see Appendix). Next, a computer program, which reads in the binary bits (9) specifying a configuration of a star, finds all possible configurations obtained by replacing 1's in (9) by 0's. To determine whether these configurations are stars or not, the degrees of the points and the graph complexity determinant[14] are computed. The star content for each modified star is finally obtained by using the recipe already described. Star contents for all seven-point stars are given in Table VIII in the Appendix. The transformation table for the seven-point Mayer stars can be accomplished in an

[14] See p. 184 of Ref. 2.

analogous manner by making a separate computer program which utilizes the five graph determinants (see Appendix). Since the table requires a large space, it was presented in a separate report.[15] Out of the 468 Mayer stars given in the Appendix, 297 stars have zero-star contents. Therefore, only 171 modified stars of different topological shapes need be considered. In the next section, these 171 modified stars are shown to depend strongly on particle dimensionality, when the particles have a hard-core potential.

III. HARD-CORE POTENTIALS

Following the convention adopted in the previous papers,[8,12] when an $\bar{f}$ function appears in a graphical expression, we denote it by a wiggly line, and we draw only these wiggly lines to represent a modified star. This convention has the advantage that a single type of wiggly-line graph can be used to represent an infinite class of the corresponding modified stars. For example,

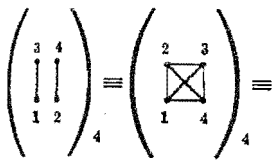

$$\equiv V^{-1}\int_V f_{12}f_{23}f_{34}f_{14}\bar{f}_{13}\bar{f}_{24}d\mathbf{r}^4,$$

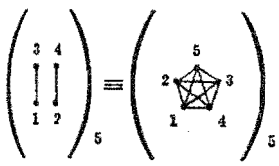

$$\equiv V^{-1}\int_V f_{12}f_{14}f_{15}f_{23}f_{25}f_{34}f_{35}f_{45}\bar{f}_{13}\bar{f}_{24}d\mathbf{r}^5.$$

In a modified star, every pair of points is connected by either an f function or an $\bar{f}$ function. When a modified star integral is evaluated for a hard-core potential, f_{ij} and $\bar{f}_{ij}$ are, respectively, -1 and 0, or 0 and 1, depending on whether r_{ij} is inside or outside the hard core. Since *each* of the distances r_{ij} in a modified star is restricted in this way the allowable configurations are severely limited. For one-dimensional hard rods, it turns out that only the complete star integral makes a nonvanishing contribution to B_n. For two-dimensional hard disks, the modified stars containing the wiggly line graphs

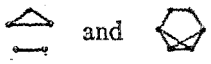

as subgraphs can be shown to give geometrically inaccessible configurations.[8] From the 171 modified star integrals in Table I, the modified stars corresponding to the following numbers in the first column of Table I contain the above graphs as subgraphs[16] and, therefore, the corresponding integrals are identically zero:

 : 4, 8, 12, 14, 16, 21, 22, 26, 27, 28, 30, 32, 34, 35, 36, 43, 44, 45, 48, 49, 50, 52, 55, 58, 59, 61, 63, 65, 66, 67, 71, 75, 77, 78, 79, 80, 81, 82, 84, 85, 86, 88, 90, 91, 92, 93, 96, 98, 101, 102, 105, 107, 108, 109, 110, 111, 113, 114, 116, 119, 121, 123, 126, 127, 128, 132, 133, 134, 136, 137, 138, 140, 144, 145, 147, 149, 152, 154, 162, 164; (10)

 : 4, 6, 8, 11, 13, 16, 17, 18, 21, 23, 25, 26, 29, 30, 33, 42, 45, 48, 56, 57, 71, 89. (11)

In addition to the above 93 modified stars, we also could not find any geometrically accessible region satisfied by the following seven-point wiggly line graphs:

10 47 76 99 (12)

The numbers under each graph correspond to the ordering for the modified stars given in Table I. As n becomes large, it becomes increasingly difficult to give a geometrical proof of inaccessibility for each individual wiggly line graph such as (12).

For a three-dimensional system of hard spheres, all modified stars containing the wiggly line graph

as a subgraph are geometrically inaccessible.[8] The following seven-point modified stars contain this subgraph, and, therefore, the corresponding integrals are zero:

 : 44, 77, 79, 108, 109, 133, 149. (13)

For a two-dimensional system of parallel hard squares and a three-dimensional system of parallel hard cubes,[17]

[15] F. H. Ree and W. G. Hoover, "Transformation Table for the Seven-Point Stars," Rept. UCRL-14634, February 1966.

[16] If a part of a wiggly line graph containing a triangular set of wiggly lines is not linked to some other part of the wiggly line graph by fewer than two intermediate wiggly lines, the wiggly line graph can be regarded as a subgraph (Ref. 8) of

Therefore, the corresponding integral also vanishes. For example,

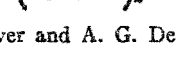

$n \geq 6$.

[17] W. G. Hoover and A. G. De Rocco, J. Chem. Phys. 36, 3141 (1962).

the exact values of modified star integrals can be evaluated by using the known integrals,[17] together with the transformation table,[15] for the seven-point stars. In addition to satisfying (11) and (12) for squares and (13) for cubes, the following seven-point modified stars in Table I for these systems give zero values of the corresponding integrals:

Squares:

2, 9, 10, 47, 70, 76, 99, 135, 150, 160, 167, 169; (14)

Cubes: 12, 162. (15)

Relations (11)–(15) can be used to express Mayer star integrals which are difficult to evaluate, such as the complete star integral, in terms of simpler Mayer star integrals. From the above discussions, at most 78 and 164 modified star integrals need to be considered in evaluating B_7 for hard disks and hard spheres, respectively. In the following section, a Monte Carlo method for evaluating these integrals is presented.

IV. MONTE CARLO INTEGRATION

Evaluation of the modified star integrals appearing in the expression for B_7 requires consideration of 18- and 12-dimensional geometry, respectively, for hard spheres and hard disks. We evaluate these integrals by a Monte Carlo method, using random trial configurations for hard spheres (disks). Particle 1 is at the origin, and the particle diameter is unit length. To make a trial configuration, Particle 2 is placed randomly within a unit sphere (circle) centered on Particle 1; Particle 3 is then placed randomly within a unit sphere (circle) centered on Particle 2, and so on. The resulting trial configuration then satisfies the conditions

$$f_{12}=f_{23}=f_{34}=f_{45}=f_{56}=f_{67}=-1. \tag{16}$$

The 15 distances between other pairs of points which are not specified by (16) are next calculated. For a pair of points separated by less than unit distance an f function is assigned; otherwise, we associate an $\bar{f}$ function with this pair. The resulting configuration may correspond to an accessible configuration of one of the modified stars in Table I. Therefore, the ith modified star integral in Table I containing m_i $(7\leq m_i\leq 21)$ f functions and $21-m_i$ $\bar{f}$ functions can be calculated by using the following recipe:

$$\text{the } i\text{th modified star integral} \equiv (-)^{m_i}(2b)^6\times[\text{fraction of Monte Carlo trial configurations (16) satisfying the geometrical restrictions of the modified star } i]/(\text{unlabeling factor of the modified star } i), \tag{17}$$

where $(-)^{m_i}(2b)^6$ is a normalizing factor and the "unlabeling factor" in (17) is the number of ways a modified star can be labeled subject to the restrictions $f_{12}=f_{23}=f_{34}=f_{45}=f_{56}=f_{67}=-1$. To determine the unlabeling factors of the modified stars in Table I, 15 binary bits (0 or 1) are chosen to specify all remaining pairs of points:

(1, 3) (1, 4) (1, 5) (1, 6) (1, 7) (2, 4) (2, 5) (2, 6)

(2, 7) (3, 5) (3, 6) (3, 7) (4, 6) (4, 7) (5, 7). (18)

The presence or absence of an f function linking any pair of points in (18) is indicated by storing either 1 or 0 in the corresponding location of the array (18). The decimal representation for the resulting binary number ranges from 0 to $2^{15}-1=32767$. A labeled modified star subject to the condition (16) corresponds to at most one of these numbers. The unlabeling factor for the modified star of the ith topological type is found by a computer program which counts the number of configurations characterized by (18) which have the same properties (number of f functions, degrees of each points, and the five graph determinants calculated in the Appendix as the modified stars of the ith type). These numbers are also listed in Table I. For a given amount of computer time, inclusion of all of these graphs improves the accuracy of the Monte Carlo value for the corresponding integral. However, three configurations cannot be built from the Monte Carlo trial configuration (16):

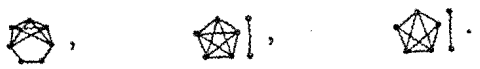

(4) (12) (27)

For hard disks, these integrals are identically zero because of Criteria (10) and (11). For hard spheres, a different type of Monte Carlo trial configuration would be required to evaluate these integrals. However, it is easy to calculate upper bounds on the absolute values of these integrals and show that the integrals are negligible for hard spheres and hard disks. From the values of the modified rooted-graph integrals occurring in the hard-sphere virial coefficient of the radial distribution function,[18] the contribution of the three integrals to B_7 can be shown not to exceed 2×10^{-6}, -6×10^{-6}, and -5×10^{-6}, respectively. The error caused by neglecting these integrals is two orders of magnitude smaller than the estimated error of B_7. Consequently, the Monte Carlo computer program ignored these integrals.

In Table I, the resulting values of the modified star integrals are given, along with their estimated errors and their contributions to B_7. These values were obtained by using 5 050 000 and 6 500 000 Monte Carlo trial configurations for hard spheres and hard disks, respectively. The errors of the Monte Carlo integrals are estimated by using the formula[19]

$$\text{error}=\left[\sum_{i=1}^{q}\frac{(\langle I_i\rangle-\langle I\rangle)^2}{q(q-1)}\right]^{1/2}, \tag{19}$$

[18] F. H. Ree, R. N. Keeler, and S. L. McCarthy, Ref. 11.

[19] G. P. Hoel, *Introduction to Mathematical Statistics* (John Wiley & Sons, Inc., New York, 1954), 2nd ed., p. 198.

TABLE II. Comparison of the various approximate values of B_7 with the exact (Monte Carlo) value of B_7 for hard spheres and hard disks.

	B_7/b^6	
	Hard spheres	Hard disks
(1) Exact	0.0138±0.0004	0.1141±0.0005
(2) Percus–Yevick (virial)[a]	17/2048=0.0083	···
(3) Percus–Yevick (OZ)[a,b]	1/64=0.0156	0.1228
(4) BGY (virial)[c]	−0.0070	0.0160
(5) BGY (OZ)[c]	−0.0217	−0.0237
(6) 1-dim. approx$\equiv B_7(\varnothing)$[d]	0.0233	0.1403
(7) 2-dim. approx[d]	0.0127	0.1141
(8) $B_7\left(\varnothing+$  $\right)$[d]	0.0118	0.1173
(9) $B_7\left(\varnothing+$  $\right)$[d]	0.0028	0.1020
(10) Padé (3, 3) approximant	0.0127	0.1149

[a] M. S. Wertheim, Phys. Rev. Letters **10**, 321 (1963); E. Thiele, J. Chem. Phys. **39**, 474 (1963); H. Reiss, H. L. Frisch, and J. L. Lebowitz, J. Chem. Phys. **31**, 369 (1959).

[b] Hard disk B_7(PY, OZ) calculated from an expression given in Table III, using the Monte Carlo values of modified star integrals given in Table I. The value of B_7 is uncertain in the last digit.

[c] F. H. Ree and B. J. Alder (unpublished result).

[d] These values are uncertain in the last digits.

where $\langle I \rangle$ is the final value of the integral I obtained from q independent smaller averages $\langle I_i \rangle$. Each of the q smaller batches contains 50 000 Monte Carlo trial configurations.

V. DISCUSSION

Just as for all the lower virial coefficients, the complete star integral is the largest modified star integral contributing to B_7 for hard spheres and hard disks. If B_7 is approximated by taking only the contribution of the complete star integral ("one-dimensional approximation" in Ref. 8) then B_7 is overestimated by 69% for hard spheres and by 23% for hard disks. In Mayer's formulation, the complete star integral makes the smallest contribution to each virial coefficient. Many of the modified star integrals shown in Table I contribute relatively little to B_7. For example, for hard spheres and hard disks, respectively, only 27 and 23 modified star integrals in Table I contribute as much as 0.001 or more to B_7. These few integrals account, respectively, for 93% and 99% of the final values of B_7. If in calculating B_7 for hard spheres, only those modified star integrals which are nonvanishing for two-dimensional hard disks are taken into account ("two-dimensional approximation" in Ref. 8), then the resulting value of B_7 is $0.0127b^6$, about 8% less than the exact value of B_7 quoted in Table I. The (3, 3) Padé approximant[8] for hard spheres also predicted $0.0127b^6$ for B_7, while the hard-disk (3, 3) Padé approximant predicted $0.1149b^6$ for B_7, which is in error by less than 1%. In Table II, various approximate values of B_7 are presented, along with the Monte Carlo values of B_7. The Percus–Yevick (PY)[20,21] virial coefficients for both hard spheres and hard disks calculated from the Ornstein–Zernike compressibility relation differ only about 13% and 8% from the exact values, while values of B_7 calculated from the Born–Green–Yvon (BGY) theory[22,23] are too small and have different signs in some cases. Rows 8 and 9 in Table II list the approximate values of B_7, obtained when only the wiggly line graph integrals which reproduce exact values of B_4 and B_5, respectively, are included in calculating B_7. These approximations are evidently poor for hard spheres and disks. If the Ornstein–Zernike compressibility relation is used to calculate the PY B_n, the resulting expression contains all star integrals which can be imbedded in a labeled n-point ring graph, subject to the condition that no two f functions can intersect within the ring. When these stars are transformed into a linear sum of the modified stars by using the transformation tables[8,15] for Mayer stars, we obtain the

[20] J. K. Percus and G. J. Yevick, Phys. Rev. **110**, 1 (1958); W. G. Hoover and J. C. Poirier, J. Chem. Phys. **38**, 327 (1963).

[21] M. S. Wertheim, Phys. Rev. Letters **10**, 321 (1963); E. Thiele, J. Chem. Phys. **39**, 474 (1963); H. Reiss, H. L. Frisch, and J. L. Lebowitz, *ibid.* **31**, 369 (1959). For two-dimensional hard disks, Reiss, Frisch, and Lebowitz's theory leads to $P/\rho kT=[1-(B_2\rho/2)]^{-2}$ [E. Helfand, H. L. Frisch, and J. L. Lebowitz, J. Chem. Phys. **34**, 1037 (1961)], with $B_n/b^{n-1}=n2^{-n+1}=0.75$, 0.5, 0.3125, 0.1875, and 0.109375 for $n=3\cdots7$. These values of B_n differ by no more than 6% from the exact values of B_n quoted in (4), (5), and Table II. Furthermore, $P/(\rho kT)$ calculated from this equation at the predicted transition density $\rho/\rho_0(=0.7622)$ is 10.49. This agrees fairly well with the observed value, 10.13 (see Table V), for a finite system of 870 hard disks.

[22] J. Yvon, *Actualités Scientifiques et Industrielles* (Hermann et Cie., Paris, 1935), Vol. 203; M. Born and H. S. Green, Proc. Roy. Soc. (London) **A188**, 10 (1946).

[23] F. H. Ree and B. J. Alder (unpublished result).

TABLE III. Virial coefficients derived from the Percus–Yevick equation using the Ornstein–Zernike compressibility relation are expressed in terms of the modified star integrals. The numbers inside the parentheses for the expression of $B_7(PY, OZ)$ correspond to ordering of modified stars given in Table I.

$nB_n(PY, OZ)$	Modified star integrals
$4B_4$	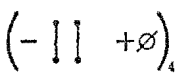
$5B_5$	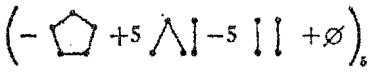
$6B_6$	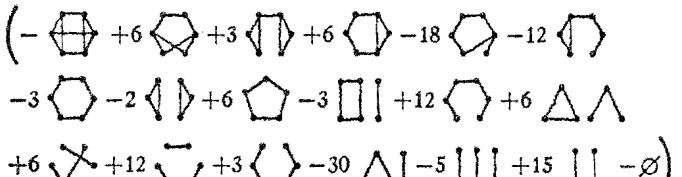
$7B_7$	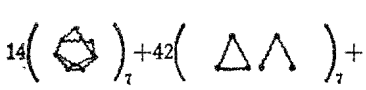

$$
\begin{aligned}
&(-1(1)+7(5)+14(7)+7(8)+7(11)-21(15)-14(18)-14(19)\\
&-7(20)-14(21)-28(22)-7(23)-7(24)-14(25)-14(26)\\
&+28(31)-7(35)+14(36)-14(37)+7(38)-7(39)+28(40)+28(41)\\
&+14(42)+7(43)+28(45)+14(46)+7(47)+28(48)+7(51)+7(52)\\
&-7(53)+7(54)+7(60)+28(61)+28(62)+14(63)+28(66)+14(67)\\
&-28(68)+21(69)-28(71)+21(72)+14(73)-14(74)-7(75)+14(77)\\
&-14(78)-56(83)-14(85)-28(86)-56(87)-28(88)-28(90)-35(93)\\
&-42(94)-28(95)-56(96)-28(98)-28(99)-28(100)-14(101)\\
&-56(102)-56(103)-14(104)-14(105)-35(106)-42(107)-14(108)\\
&-35(109)+42(112)+56(113)+7(114)-7(115)+42(117)+42(118)+21(119)\\
&+28(120)+70(122)+56(123)+28(124)+70(125)+112(126)+21(127)\\
&+42(128)+28(129)+112(130)+84(131)+140(132)+56(133)+7(134)\\
&+23(135)-126(139)-84(140)+42(141)-112(142)-84(143)-28(144)\\
&-84(145)-21(146)-14(147)-14(149)-14(150)-140(151)-56(152)\\
&-7(153)+21(155)-42(156)-21(157)+84(159)-14(160)+42(161)\\
&+7(162)+42(163)+84(165)+21(166)+42(167)-105(168)-35(169)\\
&+35(170)-1(171))_7
\end{aligned}
$$

TABLE IV. Values of $PV/(NkT)$ for hard spheres obtained by using the six-term and the seven-term virial series, the Padé approximants, and the molecular-dynamics data (MD). The Padé approximant (3, 4; ∅) is obtained by using the virial coefficients calculated from the complete star integrals alone in the reformulated expression of $B_n(n<8)$.

V/V_0	Six-term series	Seven-term series	Padé (3, 4; ∅)	Padé (3, 3)	Padé (4, 3)	MD[a]
1.5	10.46	11.27	12.63	12.31	13.21	12.5[b]
1.6	8.95	9.50	10.73	10.11	10.58	10.17
1.7	7.79	8.18	9.18	8.55	8.81	8.59
2.0	5.59	5.73	6.21	5.83	5.90	5.89
3.0	3.01	3.03	3.20	3.03	3.03	3.05
10.0	1.36	1.36	1.36	1.36	1.36	1.36

[a] The data for $V/V_0 \neq 1.5$ are obtained for a system of 108 hard spheres and were furnished by B. J. Alder and T. E. Wainwright. (Also, see Ref. 8.)

[b] At this density, both solid and fluid phases can occur, for a system of 500 hard spheres. For a system of infinite number of particles the phase transition from the fluid to the solid is estimated to start at $V/V_0 \simeq 1.5$ and have an extended flat isotherm up to $V/V_0 \simeq 1.35$.

TABLE V. Values of $PV/(NkT)$ for hard disks obtained by using the six-term and the seven-term virial series, the Padé approximants, and the molecular-dynamics data (MD). The Padé approximant $(3, 4; \varnothing)$ is obtained by using the virial coefficients calculated from the complete star integrals alone in the reformulated expression of $B_n (n<8)$.

V/V_0	Six-term series	Seven-term series	Padé $(3, 4; \varnothing)$	Padé $(3, 3)$	Padé $(3, 4)$	MD[a]
1.312[b]	7.51	8.31	12.69	10.74	10.42	10.13
1.40	6.43	6.97	9.36	8.29	8.16	8.25
1.45	5.94	6.38	8.13	7.34	7.25	7.47
1.50	5.52	5.88	7.19	6.59	6.53	6.67
1.55	5.16	5.45	6.45	5.98	5.94	6.08
1.60	4.84	5.08	5.86	5.49	5.46	5.56
1.65	4.56	4.76	5.37	5.07	5.05	5.13
1.70	4.31	4.48	4.97	4.72	4.71	4.76
1.80	3.90	4.02	4.34	4.17	4.16	4.24
1.90	3.57	3.65	3.87	3.75	3.74	3.78
2.00	3.30	3.36	3.51	3.42	3.42	3.39

[a] These data for 72 hard disks are given in W. G. Hoover and B. J. Alder, J. Phys. 46, 686 (1967); see also Ref. 8.

[b] For a periodic system of 870 hard disks the phase transition from fluid to solid starts at $V/V_0 \simeq 1.312$ and extends to $V/V_0 \simeq 1.266$. See Ref. 25. For an infinite system of hard disks the transition occurs at higher density and pressure.

reformulated expression for the PY B_n according to the Ornstein–Zernike compressibility relation as shown in Table III for $n<8$. The numbers inside parentheses in the expression for B_7 (PY, OZ) correspond to the ordering of modified stars given in Table I. Two types of modified stars appearing in the expression for B_7 (also one in B_6) in Table III do not occur in the exact expressions for B_7. However, because of conditions such as (10) and (11), these integrals vanish identically for hard disks. The calculated values of B_n(PY, OZ) $(n<8)$ for hard disks[24] are

B_n(PY, OZ):

$$B_4/b^3 = 2 - (4\sqrt{3}/\pi) + (22/3\pi^2) = 0.5377,$$

$$B_5/b^4 = 0.3433,$$

$$B_6/b^5 = 0.2092,$$

$$B_7/b^6 = 0.1228, \qquad (20)$$

where the values of B_5, B_6, and B_7 are uncertain in the last digits because of Monte Carlo integrations.

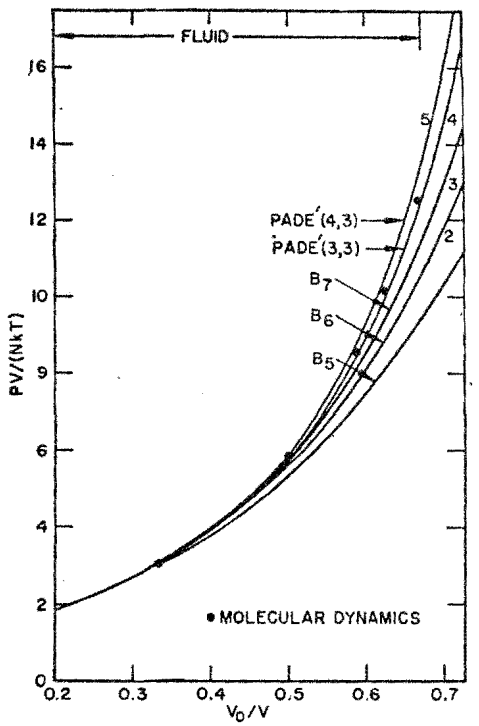

FIG. 1. Hard-sphere equations of state. The curves represent: (1) the five-term virial series, (2) the six-term virial series, (3) the seven-term virial series, (4) (3,3) Padé approximant, (5) (4,3) Padé approximant. Molecular-dynamics data (Table IV) are indicated by •••.

In Tables IV and V, the pressure is calculated by truncating the infinite virial series after six or seven terms to estimate the density range, where the virial series converges. Comparison of the truncated series with the molecular-dynamics (MD) data of Alder and Wainwright[9,25] provides empirical information on the radius of convergence of the virial series. Also included in Tables IV and V are the values of the pressure calculated from the Padé approximants.[26] A Padé approximant $P(n, m)$ to $[PV^2/(N^2kT)]-V/N$ which reproduces $m+n$ virial coefficients is obtained by dividing a polynomial in ρ of degree $n-1$ by a second polynomial of degree $m-1$. The coefficients occurring in the two polynomials are uniquely determined from known values of B_i $(i \leq n+m)$. Table VI lists $P(3, 3)$, $P(3, 4)$, and $P(4, 3)$ together with $P(3, 4; \varnothing)$, which is the Padé approximant using the values of B_n calculated from the complete star integrals alone. The approximant $P(3, 4; \varnothing)$ will, therefore, reproduce the exact B_n for $n<4$. In the case of hard spheres (Fig. 1), the seven-term virial series lies below the molecular-

[24] B_4(PY, OZ)/b^3 given in Eq. (20) is obtained by Rowlinson (Ref. 11).

[25] B. J. Alder and T. E. Wainwright, Phys. Rev. 127, 359 (1962).

[26] For a general review of the Padé approximant, we refer to G. A. Baker, in *Advances in Theoretical Physics*, K. A. Brueckner, Ed. (Academic Press Inc., New York, 1965), Vol. 1, Chap. 1.

TABLE VI. Padé approximants to $PV/(NkT)-1$ for hard spheres and hard disks. The approximant $P(n, m)$ reproduces the exact B_i for $i \leqq n+m$.

	$PV/(NkT)-1$	
	Hard spheres	Hard disks[a]
$P(3, 3)$	$\dfrac{b\rho+0.063499(b\rho)^2+0.017327(b\rho)^3}{1-0.561501(b\rho)+0.081316(b\rho)^2}$	$\dfrac{b\rho-0.202080(b\rho)^2+0.005589(b\rho)^3}{1-0.984085(b\rho)+0.242916(b\rho)^2}$
$P(3, 4)$	$\dfrac{b\rho-0.425442(b\rho)^2+0.037353(b\rho)^3}{1-1.050442(b\rho)+0.406930(b\rho)^2-0.063207(b\rho)^3}$	$\dfrac{b\rho+0.336688(b\rho)^2-0.132980(b\rho)^3}{1-0.445317(b\rho)-0.316972(b\rho)^2+0.151085(b\rho)^3}$
$P(4, 3)$	$\dfrac{b\rho+0.351862(b\rho)^2+0.086711(b\rho)^3+0.013469(b\rho)^4}{1-0.273138(b\rho)-0.029527(b\rho)^2}$	$\dfrac{b\rho-0.285277(b\rho)^2-0.007293(b\rho)^3-0.003476(b\rho)^4}{1-1.067282(b\rho)+0.295094(b\rho)^2}$
$P(3, 4; \varnothing)$	$\dfrac{b\rho-1.110356(b\rho)^2+0.134408(b\rho)^3}{1-1.735356(b\rho)+0.902280(b\rho)^2-0.156493(b\rho)^3}$	$\dfrac{b\rho+7.551170(b\rho)^2-2.252641(b\rho)^3}{1+6.769166(b\rho)-8.094814(b\rho)^2+2.254440(b\rho)^3}$

[a] The present hard disk $P(3, 3)$ differs from an expression given in Ref. 8. This is due to the use of B_4 with fewer significant figures in Ref. 8.

dynamics data but agrees closely with the MD data over a wide range of density. At $V/V_0=1.6$, for example, only 60% expanded from close packing, the difference between the two is less than 7%. Since the phase transition from the fluid phase to the solid phase is estimated to start at $V/V_0\approx1.5$,[27] this indicates that the virial series converges in the entire fluid range for a system with an infinite number of hard spheres. In the case of hard disks (Fig. 2), the seven-term virial series improves the values of the pressure calculated from the six-term virial series, but still lies 18% below the molecular-dynamics value 10.13 of PV/NkT at $V/V_0=1.312$, where the tie line for 870 hard disks intersects the fluid branch.[28] We expect, therefore, that the next few B_n's will have positive signs. The values of $PV/(NkT)$ calculated from the Padé approximants agree closely with the molecular-dynamics data for both hard spheres and hard disks over the entire fluid range.[29] However, the symmetric Padé (3, 3) approximants generally agree better than nonsymmetric ones. It is interesting to note that a hard-disk Padé approximant exhibits a maximum in the pressure at high density (therefore, occurrence of thermodynamically unstable region beyond this density). The densities, where the maxima occur for the $P(3, 3)$, $P(3, 4)$, and $P(4, 3)$ approximants, are, respectively, given by

$$\rho_{\max}=1.12\rho_0,\ 1.06\rho_0,\ \text{and}\ 0.99\rho_0,$$

where ρ_0 is the close-packed density $(\frac{4}{3})^{1/2}\sigma^{-2}$. The maxima occur because complex pairs of the zeros of the denominators in each Padé approximant lie adjacent to real positive axis located at

$$\cos\theta_{\max}=0.998,\ 0.989,\ \text{and}\ 0.982$$

in the complex ρ plane with the moduli approximately equal to $\rho_{\max}$. In the case of the hard-disk $P(3, 4)$ approximant, an additional root occurs at $\rho/\rho_0\approx-0.965$, and this root determines the radius of the convergence of the $P(3, 4)$ approximant. From the above considerations, it is tempting to conjecture that the hard-disk virial series diverges at the close-packed density and that the hard-disk virial series contains information (such as the value of ρ_0) about the high-density side. However, we need to know values of more virial coefficients to test the validity of the above conjecture. The convergence of the virial series over a certain range of

[27] The present (revised) value ($V/V_0\approx1.5$) is estimated from the molecular-dynamics data for a system of 500 hard spheres. For 500 spheres the solid phase is unstable at $V/V_0=1.5$. The value ($V/V_0\approx1.63$) earlier quoted in Ref. 8 is estimated from molecular-dynamics data for 108 hard spheres. The molecular-dynamics data were kindly furnished by B. J. Alder.

[28] This predicted phase transition may contradict the proof of instability of a solid phase with a periodic singlet distribution function in a two-dimensional continuum system [L. D. Landau and E. M. Lifshitz, *Statistical Physics* (Addison-Wesley Publ. Co., Reading, Mass., 1958), Sec. 125, cited in F. H. Stillinger, E. A. DiMarzio, and R. L. Kornegay, J. Chem. Phys. **40**, 1564 (1964)]. Whether or not hard-disk systems have a periodic singlet distribution function at high density is unknown. In a recent paper [W. G. Hoover and F. H. Ree, J. Chem. Phys. **45**, 3649 (1966)], we investigate the melting problem by employing a simple hard-core model. For this model, two- and three-dimensional systems behave quite differently. In particular, the two-dimensional model system seems to show no phase transition to an ordered state, thus supporting the argument of Landau and Lifshitz. At the same time the hard-disk transition seems well established. The number dependence of the tie line has been calculated to vary as $(1/N)\ \ln N$. This dependence agrees with the machine results and predicts only a small change from 870 disks to an infinite system [W. G. Hoover and B. J. Alder J. Chem. Phys. **46**, 686 (1967)].

[29] The coefficients appearing in the Padé approximants in Table VI are sensitive functions of the values of the virial coefficients used to calculate them. However, no significant change in calculated values occurs for entire fluid range. For example, if the upper and lower Monte Carlo values of B_5, B_6, and B_7 quoted in Eqs. (4), (5), and Table II are used, the corresponding pressures from the approximants $P(3,4)$ for hard disks are 10.34 for upper limits and 10.30 for lower limits of B_n at $\rho/\rho_0=0.76$, which is close to the density at which the phase transition starts from the fluid phase. The values of the approximants $P(4,3)$ for hard spheres, using the extremum Monte Carlo values of B_n are similarly in good agreement with the values calculated from the approximant $P(4,3)$ in Table VI.

TABLE VII. The virial coefficients for the compressibility series,

$$d\rho/d(\beta P) = \sum_{n=1}^{\infty} C_n \rho^{n-1},$$

for hard disks, hard spheres, hard parallel squares, and hard parallel cubes ($C_1 \equiv 1$). The coefficients are expressed in units of B_2 and V_0(≡the close-packed volume).

	Unit of B_2					
	C_2	C_3	C_4	C_5	C_6	C_7
Disks	−2	1.65399	−0.74487	0.198(3)[a]	−0.028(6)	0.007(3)
Spheres	−2	2.125	−1.64780	1.055(2)	−0.589(4)	0.285(6)
Squares[b]	−2	1.75	−0.83333	0.23264	−0.03941	0.00140
Cubes[b]	−2	2.3125	−1.95833	1.36928	−0.83784	0.46256
	Unit of V_0					
	C_2	C_3	C_4	C_5	C_6	C_7
Disks	−3.62760	5.44140	−4.44478	2.15(3)	$-5(1)\times10^{-1}$	$2(1)\times10^{-1}$
Spheres	−5.92385	1.86426×10	-4.28180×10	$8.12(1)\times10$	$-1.34(1)\times10^{2}$	$1.92(4)\times10^{2}$
Squares	−4	7	−6.66667	3.72222	−1.26111	8.99072×10^{-2}
Cubes	−8	37	-1.25333×10^{2}	3.50535×10^{2}	-8.57944×10^{2}	1.89466×10^{3}

[a] Numbers inside of parentheses denotes standard deviation in the last digit. For example, 0.198(3) ≡ 0.198±0.003.
[b] The values of $B_n(n<8)$ obtained in Ref. 17 are used to calculate $C_n(n<8)$.

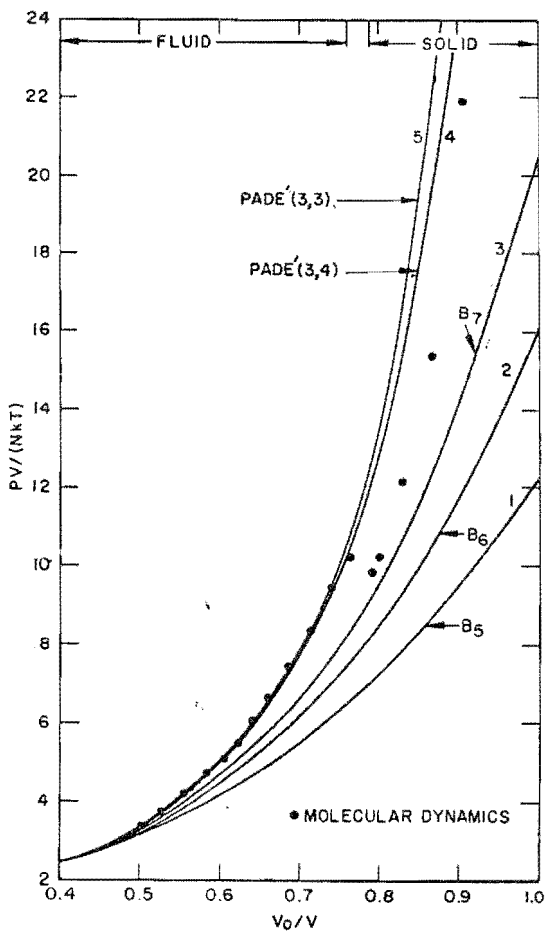

FIG. 2. Hard-disk equations of state. The curves represent: (1) the five-term virial series, (2) the six-term virial series, (3) the seven-term virial series, (4) (3,3) Padé approximant, (5) (3,4) Padé approximant. Molecular-dynamics data (Table V) are indicated by ••••.

densities does not necessarily imply that the equation of state should follow the same isotherm as the virial series.[30] In the case of the hard-sphere Padé approximants, the denominators behave less regularly. The hard-sphere $P(3, 3)$ approximant exhibits a maximum in the pressure at $\rho/\rho_0 \approx 1.19 (\rho_0 = \sqrt{2}\sigma^{-3})$, while the $P(3, 4)$ and $P(4, 3)$ approximants have poles at $\rho/\rho_0 = 0.715$ and 0.948, respectively.

The good agreement Padé approximants show with the hard-sphere and hard-disk fluid-phase isotherms and the accuracy of virial coefficients predicted by these approximants (Tables II, IV, and V) both indicate that the approximants are better approximations to exact results than any currently popular approximate theories of fluids. Values of B_8 can be estimated from the density expansion of the Padé approximants in Table VI. The resulting values of B_8 are

$$\text{Hard spheres:} \quad B_8/b^7 = 0.0058 \text{ from } P(3, 4) \quad (21a)$$
$$= 0.0049 \text{ from } P(4, 3); \quad (21b)$$
$$\text{Hard disks:} \quad B_8/b^7 = 0.0635 \text{ from } P(3, 4) \quad (22a)$$
$$= 0.0630 \text{ from } P(4, 3). \quad (22b)$$

Although the hard-sphere and hard-disk virial series appear to converge over the entire fluid range, knowledge of the several higher virial coefficients is necessary to calculate the pressure within 1% accuracy in the fluid range. The calculation of the higher B_n requires, however, the evaluation of a large number of star integrals. The number of star integrals of different topological types probably grows asymptotically as $2^{n(n-1)/2}/n!$.[31] It is, therefore, profitable to find a thermodynamic quantity whose virial series converges faster

[30] M. Kac, G. E. Uhlenbeck, and P. C. Hemmer, J. Math. Phys. 4, 216 (1963).
[31] R. J. Riddell and G. E. Uhlenbeck, J. Chem. Phys. 21, 2056 (1953).

than the usual virial series of the pressure. In the case of the one-dimensional hard rods of unit length, the equation of state[32] is given by

$$\beta P=\rho/(1-\rho). \tag{23}$$

Therefore, for the corresponding compressibility series,

$$\sum_{n=1}^{\infty} C_n\rho^{n-1},$$

$$\frac{d\rho}{d(\beta P)}=\sum_{n=1}^{\infty} C_n\rho^{n-1}=1-2\rho+\rho^2 \tag{24}$$

is a *finite* series in density. This suggests that the compressibility series for a two-dimensional system of hard particles may also exhibit a rapidly converging series. In Table VII, the values of C_n are given for various systems of hard particles, in both two and three dimensions. First, we note that the signs of the coefficients alternate in all these cases. Whether or not this holds true for larger n and for any continuum system of hard particles is an unsolved problem.[33] Second, in the cases of hard disks and hard squares, when C_n is expressed in unit of the close-packed volume, the series appear to converge rather rapidly even at the close-packed density! For example, the contributions of the various terms at $\rho/\rho_0=0.8$ are given by

Hard disks:

$$d\rho/d(\beta P)=1-2.90+3.43-2.28+0.88-0.16+0.05+\cdots, \tag{25}$$

Hard squares:

$$d\rho/d(\beta P)=1-3.2+4.48-3.41+1.52-0.41+0.02+\cdots. \tag{26}$$

Since C_n rapidly decreases as n (<8) increases, an alternative estimate of B_8 for hard disks and hard squares can be obtained from the virial series of $d\rho/d(\beta P)$ by setting $C_n=0$ for $n>7$. The estimated values of B_8 are

$$\text{Hard disks:}\quad B_8/b^7=0.0616\pm0.0001, \tag{27}$$

$$\text{Hard squares:}\quad B_8/b^7=-0.000352. \tag{28}$$

The errors quoted in Eq. (27) and Table VII are estimated from the appropriate values calculated by using the upper and lower bounds of the Monte Carlo values of B_n ($n>4$) for hard spheres and hard disks. Unfortunately, for a three-dimensional system of hard particles, the compressibility series shows slower convergence than the usual virial series of the pressure; therefore, no advantage will be gained by using the virial series of the compressibility in the case of three-dimensional hard particles.

ACKNOWLEDGMENT

We are grateful to Warren G. Cunningham for his assistance in programming the Monte Carlo integrations for the CDC 3600 computers at Livermore.

APPENDIX

A star with a given topological type can be characterized by assigning to it a set of invariant numbers which are independent of labeling the star. For seven-point stars, we were unable to find a single convenient invariant quantity which differentiates all 468 topologically different stars. Therefore, we resort to the following set of numbers to classify the seven-point stars with different topological shapes:

(1) l is the number of f functions in a star;

(2) $d_i (i = 1, 2, \cdots, 7)$ is the *degree* at each of the seven points in a star (the degree at a point is defined as number of f functions which terminate at the point);

(3) D_1 = the graph complexity determinant, a 6×6 determinant whose elements are obtained from the following rule: for $i\neq j$, if there is an f function, $(D_1)_{ij}=1$; otherwise, $(D_1)_{ij}=0$; for $i=j$,

$$(D_1)_{ii}=-\sum_{j=1,(j\neq i)}^{7}(D_1)_{ij}, \qquad (i=1, 2, \cdots, 7);$$

the D_1 is a 6×6 determinant obtained by eliminating any one of the seven rows and the corresponding column of $(D_1)_{ij}$[34];

(4) D_2 is a 7×7 determinant whose off-diagonal elements $(D_2)_{ij}$ are the same as $(D_1)_{ij}$, but

$$(D_2)_{ii}=\sum_{j=1,i\neq j}^{7}(D_1)_{ij}, \qquad (i=1, 2, \cdots, 7);$$

(5) D_3 is the absolute value of a 7×7 determinant whose off-diagonal elements $(D_3)_{ij}$ are the same as $(D_1)_{ij}$, but $(D_3)_{ii}=0$, $(i=1, 2, \cdots, 7)$;

(6) D_4 is the absolute value of a 7×7 determinant whose off-diagonal elements are the compliments of $(D_1)_{ij}$ [i.e., $(D_4)_{ij}\equiv1-(D_1)_{ij}$], and the diagonal elements $(D_4)_{ii}=0$, $(i=1, 2, \cdots, 7)$;

(7) D_5 is a 7×7 determinant whose off-diagonal elements $(D_5)_{ij}$ are the same as $(D_4)_{ij}$, but

$$(D_5)_{ii}=\sum_{j=1}^{7}(D_4)_{ij}, \qquad (i=1, 2, \cdots, 7).$$

In Table VIII, D_1, D_2, D_3, and D_4 are listed for each of the 468 seven-point Mayer stars.[35] Since the use of

[32] K. F. Herzfeld and M. G. Mayer, J. Chem. Phys. **2**, 38 (1934).

[33] For a hard lattice gas, the coefficients given by D. S. Gaunt and M. F. Fisher [J. Chem. Phys. **43**, 2840 (1965)] do *not* alternate in sign.

[34] The elements for the graph complexity determinant defined in this manner have signs opposite to those used in Ref. 2.

[35] The diagrams for these 468 Mayer stars are taken from Ref. 17.

TABLE VIII. Labeling factors, star contents $\tilde{a}(\equiv\tilde{a}[7])$ and values of various graph determinants to be used to characterize the seven-point Mayer stars.

I	Graph	Label	D_1	D_2	D_3	D_4	$\tilde{a}$
1		-360	7	4	2	4	1
2		2520	17	24	4	0	0
3		2520	19	16	0	6	0
4		1260	20	0	0	0	1
5		1260	21	24	4	0	1
6		-1260	36	80	0	0	0
7		-5040	37	92	2	0	0
8		-1260	39	60	2	0	0
9		-2520	39	108	6	0	0
10		-2520	39	140	6	0	0
11		-2520	40	64	0	8	0
12		-5040	41	60	2	2	0
13		-2520	41	60	0	0	0
14		-420	44	48	0	8	1
15		-1260	40	80	8	0	-2
16		-2520	44	0	0	2	0
17		-5040	43	92	2	2	0
18		-2520	44	80	0	2	0
19		-1260	44	80	0	2	0
20		-630	48	64	0	12	1
21		-5040	46	80	0	0	-2
22		-1260	48	48	0	10	-1
23		-840	50	0	0	0	-2
24		-840	49	108	6	6	-2
25		-2520	51	60	2	8	-1
26		21	80	0	0	4	1
27		420	68	192	0	2	0
28		2520	72	176	0	2	0
29		5040	73	224	0	2	0
30		2520	76	256	0	0	0
31		1260	76	320	0	2	0
32		2520	75	216	4	2	0
33		840	84	128	0	0	0
34		5040	76	224	0	0	0
35		5040	76	224	2	2	0
36		1260	72	240	5	0	0
37		1260	80	192	0	2	0
38		5040	79	264	4	0	0
39		5040	79	296	4	0	0
40		5040	79	344	2	0	0
41		2520	81	336	8	0	0
42		1260	80	240	2	0	0
43		2520	84	176	0	2	0
44		2520	84	176	0	2	0
45		1260	84	224	0	0	0
46		2520	85	272	0	2	0
47		2520	85	240	0	0	0
48		5040	82	264	2	2	0
49		1260	84	192	0	12	0
50		5040	85	176	0	2	0
51		2520	88	176	2	0	0
52		1260	88	240	2	0	-2
53		630	96	0	0	4	-1
54		2520	88	336	10	0	0
55		1260	88	400	8	0	0
56		5040	89	224	0	6	0
57		2520	90	200	0	2	0
58		2520	87	264	8	0	3
59		2520	93	144	0	0	0
60		2520	91	264	4	0	0
61		2520	96	176	0	8	-2
62		2520	96	144	0	2	0
63		5040	94	264	0	0	0
64		5040	94	296	2	2	0
65		1260	96	256	0	0	-2
66		2520	93	240	0	2	1
67		2520	95	200	4	0	3
68		1260	96	256	0	0	3
69		5040	98	264	2	2	1
70		5040	101	176	0	8	1
71		1260	105	0	0	0	0
72		2520	104	224	2	8	-1
73		1260	105	336	0	4	4
74		2520	110	200	2	2	2
75		630	117	144	0	12	3
76		-21	112	320	0	0	0
77		-840	124	464	0	0	0
78		-630	128	512	0	0	0
79		-1260	132	560	0	2	0
80		-2520	136	624	0	2	0
81		-2520	136	560	0	0	0
82		-2520	135	580	2	0	0
83		-2520	135	612	2	2	0
84		-630	144	384	0	0	0
85		-1260	136	528	0	0	0
86		-210	160	320	0	0	-2
87		-5040	141	660	6	0	0
88		-5040	144	720	2	0	0
89		-2520	144	640	4	0	0
90		-2520	144	768	0	0	0
91		-5040	139	516	2	0	0
92		-1260	140	528	0	0	0
93		-2520	148	512	0	2	0
94		-2520	144	528	2	0	0
95		-5040	151	516	2	2	0
96		-630	160	384	0	0	0
97		-2520	160	464	0	2	0
98		-2520	154	560	0	0	0
99		-2520	152	688	8	0	0
100		-1260	152	880	0	0	0
101		-2520	153	580	2	2	0
102		-2520	156	528	0	2	0
103		-2520	155	612	2	4	0
104		-1260	160	704	0	0	0
105		-2520	160	672	2	0	0
106		-5040	159	612	2	2	0
107		-5040	159	580	0	0	0
108		-1260	160	512	0	0	0
109		-2520	168	592	0	0	0
110		-2520	156	528	0	4	0
111		-5040	162	688	4	0	0
112		-5040	162	736	2	0	0
113		-5040	163	580	2	2	0
114		-2520	155	612	8	0	0
115		-2520	159	516	2	0	0
116		-2520	168	800	2	0	0
117		-2520	168	736	4	0	0
118		-1260	168	784	12	0	0
119		-2520	171	420	0	2	0
120		-5040	166	640	0	0	0

TABLE VIII (*Continued*)

I	Graph	Label	D_1	D_2	D_3	D_4	$\tilde{a}$
121		-1260	180	384	0	2	1
122		-5040	172	528	0	2	0
123		-2520	168	640	0	4	0
124		-5040	169	660	6	0	0
125		-1260	165	612	0	2	3
126		-5040	175	516	0	4	0
127		-1260	175	420	2	0	0
128		-2520	171	580	2	0	0
129		-1260	180	560	0	2	3
130		-5040	178	624	0	0	0
131		-5040	177	820	8	0	0
132		-2520	176	512	0	8	0
133		-2520	176	640	8	0	-4
134		-2520	184	384	0	2	1
135		-2520	183	612	0	0	0
136		-2520	183	708	0	2	0
137		-5040	181	580	2	2	3
138		-1260	189	420	0	6	4
139		-630	192	384	0	0	2
140		-2520	187	580	0	2	-1
141		-2520	190	720	0	4	0
142		-2520	192	688	2	0	4
143		-2520	185	756	8	2	-1
144		-630	192	960	12	0	4
145		-5040	191	580	2	2	-1
146		-1260	195	756	0	0	0
147		-5040	194	688	0	0	-1
148		-5040	199	420	0	2	0
149		-5040	196	640	2	2	2
150		-1260	195	612	0	0	0
151		-2520	205	612	0	8	3
152		-630	207	324	0	0	0
153		-420	216	0	0	4	4
154		-2520	204	528	0	10	1
155		-2520	209	820	2	2	-2
156		-1260	224	640	4	0	1
157		-1260	231	420	0	8	-1
158		210	224	960	0	0	0
159		2520	236	1104	0	0	0
160		630	240	1152	0	0	0
161		2520	248	1264	2	0	0
162		840	242	1176	0	0	0
163		840	243	1200	0	0	0
164		2520	245	1224	4	0	0
165		1260	256	1344	0	0	0
166		1260	264	1104	0	0	0
167		5040	257	1336	4	0	0
168		5040	257	1384	2	0	0
169		2520	260	1440	0	0	0
170		1260	264	1456	10	0	0
171		2520	272	1504	4	0	0
172		2520	272	1696	4	0	0
173		1260	273	1176	0	0	0
174		1260	255	1152	0	0	0
175		2520	272	1216	2	0	0
176		1260	276	1344	0	2	0
177		2520	260	1152	2	0	0
178		2520	276	1120	2	0	0
179		630	300	960	0	2	3
180		5040	278	1336	2	2	0
181		5040	281	1384	2	2	0
182		5040	279	1216	0	0	0
183		630	288	1152	0	0	0
184		2520	291	1104	0	2	0
185		2520	288	1344	0	0	0
186		2520	288	1440	0	2	0
187		5040	284	1216	0	0	0
188		2520	285	1224	4	0	0
189		2520	287	1456	8	0	0
190		1260	288	1536	0	2	0
191		1260	300	1104	0	0	0
192		2520	296	1120	0	2	0
193		5040	289	1336	4	0	0
194		315	320	1280	0	0	4
195		2520	297	1400	2	0	0
196		420	275	1296	8	0	-6
197		2520	296	1360	2	0	0
198		5040	297	1576	2	0	0
199		5040	299	1264	0	2	0
200		2520	305	1704	2	0	0
201		2520	305	1560	8	0	0
202		630	320	1536	0	0	0
203		2520	308	1600	8	2	0
204		2520	315	1488	0	0	0
205		2520	315	1360	2	2	0
206		2520	320	1568	4	0	0
207		420	324	864	0	0	0
208		1260	320	1856	2	0	0
209		2520	308	1344	6	0	0
210		5040	321	1384	2	2	0
211		630	320	1024	0	6	-3
212		420	320	1536	12	0	5
213		1260	315	1200	0	0	-6
214		5040	313	1464	8	0	0
215		5040	324	1504	0	0	0
216		5040	320	1216	2	2	0
217		5040	324	1216	0	0	0
218		5040	326	1464	0	0	0
219		2520	323	1360	0	4	0
220		5040	329	1576	2	2	0
221		5040	339	1264	0	2	-1
222		2520	330	1400	2	2	-4
223		2520	327	1344	0	2	-4
224		2520	336	1152	0	2	0
225		840	351	864	0	2	-4
226		2520	335	1680	8	0	0
227		1260	336	1152	0	4	-1
228		630	325	1512	12	0	-4
229		1260	345	1368	0	0	0
230		2520	344	1120	0	2	-2
231		5040	338	1464	2	2	-5
232		1260	360	1488	0	0	-2
233		2520	340	1344	2	0	-4
234		1260	352	1408	0	0	-1
235		5040	354	1336	0	2	-6
236		1260	360	864	0	0	-4
237		5040	353	1656	6	0	1
238		1260	360	1904	10	0	-6
239		2520	355	1360	0	6	-5
240		840	361	1800	0	0	0

I	Grap
241	
242	
243	
244	
245	
246	
247	
248	
249	
250	
251	
252	
253	
254	
255	
256	
257	
258	
259	
260	
261	
262	
263	
264	
265	
266	
267	
268	
269	
270	
271	
272	
273	
274	
275	
276	
277	
278	
279	
280	

TABLE VIII (*Continued*)

I	Graph	Label	D_1	D_2	D_3	D_4	$\tilde{a}$
241		2520	368	1344	0	0	0
242		2520	372	1344	0	2	-2
243		2520	368	1824	8	2	-4
244		2520	377	1624	0	0	0
245		5040	386	1656	0	0	-5
246		1260	385	1560	2	0	-2
247		1260	399	1440	0	8	-6
248		840	392	1536	6	6	-8
249		1260	408	864	0	2	-5
250		2520	400	1216	0	6	-4
251		35	432	0	0	6	-17
252		-630	420	2160	0	0	0
253		-315	448	2560	2	0	0
254		-1260	429	2268	0	0	0
255		-1260	440	2448	0	0	0
256		-5040	441	2460	2	0	0
257		-2520	444	2496	2	0	0
258		-420	425	2268	0	0	0
259		-2520	451	2604	6	0	0
260		-1260	455	2604	6	0	0
261		-2520	456	2688	0	0	0
262		-2520	465	2748	0	0	0
263		-2520	472	2848	4	0	0
264		-630	480	3072	6	0	0
265		-2520	480	2928	2	0	0
266		-2520	480	3072	4	0	0
267		-210	500	2160	0	0	-6
268		-1260	480	2304	0	0	0
269		-5040	497	2620	2	0	0
270		-2520	485	2460	2	0	0
271		-840	513	2268	0	0	0
272		-630	512	3520	6	0	0
273		-2520	506	2800	0	0	0
274		-5040	512	2800	2	0	0
275		-1260	504	2496	0	0	0
276		-1260	528	2928	0	0	0
277		-420	540	2160	0	2	-4
278		-2520	513	2780	0	0	0
279		-5040	516	2880	2	0	0
280		-1260	528	2496	0	0	0
281		-2520	516	2496	2	0	0
282		-840	525	3132	2	0	0
283		-5040	523	3020	8	0	0
284		-2520	528	3200	0	0	0
285		-5040	521	2652	2	0	0
286		-1260	540	2496	2	0	0
287		-2520	537	2748	0	2	0
288		-1260	528	2816	8	0	0
289		-5040	542	2848	2	2	0
290		-1260	560	2560	0	2	-5
291		-5040	545	2620	0	0	0
292		-1260	552	3472	0	0	0
293		-1260	544	2816	0	2	0
294		-2520	545	2652	0	0	0
295		-2520	552	2944	0	2	0
296		-2520	560	3200	10	0	0
297		-5040	558	3104	2	0	0
298		-2520	560	2928	2	0	0
299		-2520	545	2844	8	0	8
300		-630	600	3120	0	0	-6
301		-1260	560	2496	0	0	2
302		-1260	576	2816	2	0	0
303		-1260	576	2304	0	2	4
304		-630	575	3276	6	0	0
305		-5040	569	2780	2	0	8
306		-2520	585	2460	0	0	4
307		-1260	585	2940	0	0	5
308		-1260	600	3552	4	0	0
309		-2520	584	2688	0	4	3
310		-2520	585	3132	2	2	0
311		-5040	593	3068	4	0	0
312		-2520	612	2928	0	2	1
313		-1260	612	2496	0	0	0
314		-5040	608	3440	2	0	0
315		-105	648	1728	0	0	6
316		-1260	608	2816	0	0	11
317		-2520	615	3500	8	2	7
318		-2520	620	3312	10	0	6
319		-5040	633	3164	0	0	2
320		-2520	638	3344	4	0	1
321		-2520	657	2748	0	2	5
322		-2520	644	3200	2	2	8
323		-5040	641	3068	2	2	7
324		-2520	644	2816	0	0	7
325		-2520	656	2496	0	2	5
326		-2520	663	3596	6	0	9
327		-1260	665	3420	0	0	10
328		-1260	680	3072	0	0	4
329		-1260	672	3456	0	4	16
330		-2520	689	3132	0	4	12
331		-210	720	1728	0	0	18
332		-630	704	2304	0	4	13
333		210	700	4320	0	0	0
334		1260	715	4536	4	0	0
335		420	756	4320	0	0	0
336		630	720	4608	0	0	0
337		1260	784	4800	2	0	0
338		840	775	5400	6	0	0
339		1260	792	4896	0	0	0
340		5040	799	5016	2	0	0
341		630	840	5520	0	0	0
342		1260	816	5280	8	0	0
343		5040	823	5336	2	0	0
344		2520	828	5504	4	0	0
345		2520	855	5016	2	0	0
346		1260	880	6240	6	0	0
347		2520	856	5024	0	0	0
348		1260	864	5120	0	0	0
349		1260	840	4896	2	0	0
350		420	864	4608	0	0	0
351		5040	871	5336	2	0	0
352		1260	880	5376	0	0	0
353		1260	897	5376	0	0	0
354		1260	900	4800	0	0	8
355		105	945	4320	0	0	5
356		2520	876	5024	2	0	0
357		2520	895	5784	2	0	0
358		5040	928	5696	2	0	0
359		2520	935	5896	8	0	0
360		1260	928	5632	0	2	0

TABLE VIII (*Continued*)

I	Graph	Label	D_1	D_2	D_3	D_4	$\tilde{a}$
361		1260	912	5280	6	0	-12
362		2520	960	5376	0	0	0
363		2520	943	6104	0	0	0
364		2520	936	5024	0	0	-4
365		1260	960	6400	0	0	0
366		315	960	5120	0	4	4
367		210	1000	6480	0	0	12
368		1260	1005	5520	0	2	7
369		1260	975	6216	12	0	-10
370		2520	986	5896	2	0	0
371		2520	984	5408	2	0	0
372		5040	1015	6424	2	0	0
373		2520	1008	5824	2	0	-10
374		1260	1020	6144	4	0	0
375		630	1024	5120	0	0	-5
376		2520	1020	6144	2	0	-2
377		1260	1045	6160	0	0	8
378		2520	1027	6264	8	0	-11
379		2520	1048	5792	0	2	-4
380		2520	1053	6032	2	2	-3
381		2520	1032	5952	6	0	-11
382		5040	1056	5696	0	0	-5
383		630	1080	4896	0	0	-4
384		1260	1056	5120	0	0	-6
385		2520	1095	6504	4	0	-4
386		2520	1102	6600	2	2	-14
387		2520	1104	6336	0	0	-16
388		2520	1128	5792	0	2	-12
389		420	1152	4608	0	2	-19
390		105	1200	5760	0	0	-12
391		360	1183	6728	4	2	-22
392		-1260	1260	8640	2	0	0
393		-35	1323	8100	0	0	0
394		-2520	1284	9024	2	0	0
395		-420	1296	9216	6	0	0
396		-1260	1320	9600	4	0	0
397		-315	1344	8960	0	0	0
398		-210	1400	10800	12	0	0
399		-2520	1368	9344	0	0	0
400		-1260	1407	9540	0	0	0
401		-1260	1392	9856	0	0	0
402		-840	1445	10164	6	0	0
403		-840	1404	9024	2	0	0
404		-1260	1463	10340	2	0	0
405		-630	1440	8960	0	0	-12
406		-2520	1488	10880	4	0	0
407		-1260	1495	10500	0	0	-10
408		-630	1575	9540	0	0	0
409		-1260	1536	9984	0	0	0
410		-5040	1543	10244	2	0	0
411		-2520	1572	10816	2	0	0
412		-2520	1600	11280	2	0	0
413		-1260	1615	10340	0	0	-11
414		-630	1584	9984	4	0	0
415		-2520	1615	11044	8	0	15
416		-2520	1648	10304	0	0	5
417		-1260	1675	11460	0	0	-14
418		-840	1682	11616	0	0	0
419		-5040	1687	11236	2	0	4
420		-2520	1692	10816	2	0	6
421		-1260	1720	10880	0	2	-7
422		-1260	1728	9984	0	0	2
423		-420	1728	11520	0	0	20
424		-140	1728	9216	0	0	6
425		-315	1800	11520	4	0	-4
426		-70	1792	9216	0	0	20
427		-252	1805	12100	0	2	5
428		-2520	1807	11716	2	0	11
429		-420	1840	10560	0	2	13
430		630	2016	15360	0	0	0
431		840	2052	16000	4	0	0
432		210	2205	16200	0	0	0
433		105	2160	15360	0	0	24
434		1260	2261	17160	2	0	0
435		630	2304	17920	4	0	0
436		1260	2345	18600	6	0	0
437		1260	2408	17760	0	0	0
438		2520	2465	18920	0	0	0
439		2520	2472	18400	2	0	0
440		1260	2520	17760	0	0	15
441		252	2527	19360	8	0	-20
442		1260	2580	19040	0	0	18
443		315	2625	19800	0	0	20
444		420	2592	17920	2	0	12
445		2520	2640	19520	2	0	-5
446		420	2688	17920	0	0	0
447		1260	2755	20240	0	0	14
448		1260	2760	19680	2	0	6
449		105	2800	19200	0	2	20
450		-105	3024	25600	6	0	0
451		-420	3528	28800	0	0	0
452		-1260	3612	30400	4	0	0
453		-105	3675	31500	10	0	0
454		-420	3780	30400	0	0	-30
455		-1260	3857	31900	0	0	0
456		-210	3920	30400	0	0	-20
457		-1260	4025	32700	0	0	-25
458		-630	4032	32000	2	0	-20
459		-315	4200	33600	0	0	-50
460		140	5292	48000	6	0	0
461		35	5488	48000	0	0	0
462		420	5635	51000	4	0	0
463		630	5880	52000	0	0	40
464		105	6125	54000	0	0	80
465		-105	8232	80000	4	0	0
466		-105	8575	82500	0	0	60
467		21	12005	125000	0	0	0
468		-1	16807	56428	6	0	120

l, d_i, D_1, D_2, D_3, and D_4 can distinguish completely all seven-point Mayer stars except the two Mayer stars corresponding to star numbers 65 and 68, in the first column of Table VIII we omitted D_5. These two stars are distinguishable since the values of D_5 for the Mayer stars 65 and 68 are, respectively, 612 and 756. Table VIII also includes number of labeling (+ sign for even number of f functions appearing in a star and − sign for odd numbers of f functions) and the star contents $\tilde{a}[7]$ of each seven-point Mayer star.

THE JOURNAL OF CHEMICAL PHYSICS VOLUME 46, NUMBER 11 1 JUNE 1967

Solution Properties of Synthetic Polypeptides. III. Viscosity Behavior of Poly-γ-Benzyl-L-Glutamate in the Helix–Coil Transition Region

AKIO TERAMOTO, KOICHI NAKAGAWA, AND HIROSHI FUJITA
Department of Polymer Science, Osaka University, Toyonaka, Japan
(Received 24 October 1966)

Limiting viscosity numbers $[\eta]$ and specific rotations $[\alpha]_{578}$ of five samples of poly-γ-benzyl-L-glutamate (PBLG) (ranging in weight-average molecular weight $\bar{M}_w$ from 1.9×10^4 to 4.0×10^5) in mixtures of dichloroacetic acid (DCA) and ethylene dichloride (EDC) of various compositions were measured as functions of temperature in the range where the PBLG molecule underwent a thermal transition from a disordered, random-coil state to an ordered helical state. For one sample the measurements of optical rotatory dispersion were made at various solvent compositions and temperatures, and the data were analyzed in terms of the Moffitt plot. When the $\bar{M}_w$ of a given sample was above a certain critical value, $[\eta]$ first decreased (or was kept constant), passed through a shallow minimum, and then increased sharply to a limiting value as the temperature was raised. Below the critical value, the change in $[\eta]$ with temperature was a monotonic decrease. Irrespective of the molecular weight of the sample, $[\alpha]_{578}$ increased sharply in a narrow range near 30°C and then gradually leveled off as the temperature was raised. This narrow region coincided with the region where $[\eta]$ underwent a marked increase. It was found that the helical content f_H of a given sample can be evaluated from the reduced mean residue rotation measured at 578 mμ. When the values of $[\eta]$ obtained under different solvent compositions and temperatures are plotted against the f_H values so calculated, the plotted points formed a single composite curve over the entire range of f_H. This curve exhibits a quite similar character to the theoretical curves for $\langle S^2\rangle$ (mean-square radius of gyration) vs f_H calculated by Nagai on the statistical-mechanical treatment of helix-forming polypeptides.

I. INTRODUCTION

IT is well known that some polypeptides change their molecular conformation from a disordered coiled state to an ordered helical state upon suitable changes in the external conditions such as solvent composition or temperature. Current statistical-mechanical theories[1–4] all argue that such a conformational transition from coil to helix proceeds through intermediate stages called interrupted helix. Nagai[5,6] was the first to calculate the change in the mean-square radius of gyration $\langle S^2\rangle$ of a polypeptide molecule accompanying the change in its helical content, and this similar problem has been treated in more detail by subsequent workers.[7] These theoretical studies predict that when the contour length of a helix-forming polypeptide molecule is above a certain critical value, $\langle S^2\rangle$ (or the mean-square end-to-end distance $\langle R^2\rangle$) first decreases, passes through a minimum, and then increases toward the value for a straight rod as the helical content of the molecule increases from zero to unity, whereas the corresponding change in $\langle S^2\rangle$ (or $\langle R^2\rangle$) for a molecule whose chain length is shorter than the critical value is a simple, monotonic decrease. Fragmentary data which demonstrated the validity of these predictions can be found in the literature,[8–10] but no systematic study, in which the effect of molecular weight is explicitly examined, appears to have been reported.

The present paper reports experimental data for the variation of $[\eta]$ accompanying the thermally induced helix-coil transition of poly-γ-benzyl-L-glutamate (PBLG) in a solvent composed of dichloroacetic acid (DCA) and ethylene dichloride (EDC). The limiting viscosity number $[\eta]$ was chosen because the change in $\langle S^2\rangle$ is expected to be most directly reflected on the change in this quantity. The data were first obtained on five PBLG samples covering a wide range of molec-

[1] J. H. Gibbs and E. A. DiMarzio, J. Chem. Phys. **30**, 271 (1959).
[2] B. H. Zimm and J. K. Bragg, J. Chem. Phys. **31**, 526 (1959).
[3] L. Peller, J. Phys. Chem. **63**, 1194, 1199 (1959).
[4] S. Lifson and A. Roig, J. Chem. Phys. **34**, 1963 (1961).
[5] K. Nagai, J. Phys. Soc. Japan **15**, 407 (1960).
[6] K. Nagai, J. Chem. Phys. **34**, 887 (1961).
[7] W. G. Miller and P. J. Flory, J. Mol. Biol. **15**, 298 (1965).
[8] P. Doty, A. Wada, J. T. Yang, and E. R. Blout, J. Polymer Sci. **23**, 851 (1957).
[9] R. Sakamoto, J. Chem. Soc. Japan Pure Chem. Sect. **85**, 17 (1964).
[10] O. B. Ptitsyn and A. M. Skvortsov, Mol. Biophys. USSR **10**, 909 (1965).